



Recent Advances in Metal–Organic Frameworks Based on Electrospinning for Energy Storage

Shunyu Yao^{1,2} · Seeram Ramakrishna² · Gang Chen¹

Received: 19 November 2022 / Accepted: 28 March 2023 / Published online: 20 June 2023
© Donghua University, Shanghai, China 2023

Abstract

Metal–organic frameworks are linked by different central organic ligands and metal-ion coordination bonds to form periodic pore structures and rich pore volumes. Because of their structural advantages, metal–organic frameworks are considered to be one of the most promising candidates for new energy storage materials. To better utilize their advantages, metal–organic frameworks can be combined with electrospinning technology to effectively adjust the porosity and mechanical strength of composite materials. This paper summarizes the combination of the latest metal–organic frameworks and classical spinning technology, starting from the structural design of electrode materials, and applying them to supercapacitors, lithium-ion batteries, lithium–sulfur batteries, sodium-ion batteries, and potassium-ion batteries. Finally, the problems and challenges related to the preparation of metal–organic framework nanofibers are summarized, and future development trends are predicted.

Keywords Metal–organic frameworks (MOFs) · Supercapacitors · Electrospinning · Lithium-ion batteries · Sodium-ion batteries

Introduction

In recent years, the rapid growth of the worldwide population has led to the increasing consumption of energy. At the same time, the consumption of fossil fuels has caused a significant increase in the emissions of carbon dioxide and other greenhouse gases, which has aggravated global climate change and environmental pollution. Because of the above-mentioned problems, it is very urgent to find a clean and environmentally friendly energy storage material to address environmental pollution and the energy crisis [1–3]. The United Nations Sustainable Development Goals were laid out in 2015, and refer to “ensuring access to affordable,

reliable and sustainable modern energy for all”. This view fully illustrates the importance of sustainable energy to the production and life of people around the world. Reducing the cost of energy materials, improving the safety of materials, and selecting materials with abundant reserves are important guarantees for the development of sustainable energy materials [4–6]. Therefore, selecting sustainable energy materials with excellent physical and chemical properties, such as porous carbon materials, porous polymers, and metal–organic frameworks (MOFs), can lead to the development of energy storage devices with excellent performance according to the need and minimize pollution in the process [7–12].

MOFs are periodic network structures comprised of metal ions and organic ligands, which have developed rapidly in recent years [13–16]. After Yaghi’s group synthesized the first MOF in the 1990s, researchers prepared zero-, one-, two- and three-dimensional MOFs with different structures by changing the central metal and organic ligand, using solvothermal, microwave thermal, and electrochemical methods and so on [17–22]. At present, more than 20,000 cases of MOFs have been reported, which have the advantages of unique structure and easy control of porosity [23–36]. In addition, MOFs act as precursors to yield a range of carbon material heterogeneities, metal oxides, and metal sulfides

✉ Seeram Ramakrishna
seeram@nus.edu.sg

✉ Gang Chen
gchen@hit.edu.cn

¹ MIIT Key Laboratory of Critical Materials Technology for New Energy Conversion and Storage, School of Chemistry and Chemical Engineering, Harbin Institute of Technology, Harbin 150001, People’s Republic of China

² Center for Nanotechnology and Sustainability, Department of Mechanical Engineering, National University of Singapore, Singapore 119260, Singapore

through heat treatment [37–39]. In general, the structure of MOFs is well preserved in the pyrolysis process [40–43]. Therefore, both MOFs and their derived materials have the advantages of high surface area, ordered multistage porosity, and controlled synthesis structures, which are conducive to exhibiting excellent performance in the electrochemical field [44]. However, a single MOF material has difficulty meeting the requirements of practical applications [45–47]. Therefore, by combining MOFs with other functional materials, the advantages of the two materials are complemented. When appropriate polymers and necessary molding technologies are introduced into MOFs, polymers can not only serve as adhesives, and enhance the mechanical properties of composite materials, but also ensure the chemical stability of materials. The as-obtained composites retain the characteristics of uniform porosity and flexibility, which can effectively expand the application range [48–51].

Electrospinning is one way to better combine MOFs with polymers. This is a mature electro-spray process that enables the large-scale preparation of micro-/nanofibers by adjusting the size of the needle. Since the sixteenth century, Gilberts claim that liquids have electrostatic attraction [52, 53]. Figure 1 demonstrates briefly the development of electrospinning [54–59]. After 500 years of development until 2000, the research focus of electrospinning technology changed from simple preparation technology to the principle and mechanism of electrospinning technology. Therefore, electrospun fiber can better regulate the size, structure, composition, morphology, and porosity of electrospun materials [60, 61].

In conclusion, the development of electrospinning in the early twenty-first century has the following characteristics: (1) plenty of polymers’ heterostructure has been obtained via electrospinning; (2) the morphology control ability of electrospun nanofibers is enhanced; (3) multicomponent inorganic composite fibers can be developed; (4) the research focus is on industrial production that can optimize the process [62–66]. Common methods for constructing fiber structures are as follows: (1) Electrospinning composite nanofibers form by adding the need material directly into the electrospinning solution [67–69]. (2) Special structure, such as core-shell, tube-in-tube, multicore cable-like, rice grain shape, helical, ribbon-like, necklace-like, multichannel tubular, nanowire-microtube, firecracker shape, and hollow fiber structures [70–84]. (3) Nanofiber composites with controllable fiber diameter and personal material properties were prepared [85, 86]. To further study the development trend of MOFs and electrospinning, the two keywords were searched. MOF material was first reported in 1977. The electrospinning technique was first reported by Xiong in 1997. The quantity and quality of research papers on electrospinning and MOFs have improved since the twenty-first century. Electrospinning and metal-organic frameworks both increased from only a few papers per year to 5583 and 7483 in 2022 (Fig. 2) [87–91]. In the reported literature, polymer nanofibers can become the most ideal framework for MOF materials because of their large specific surface area, high porosity, high mechanical strength, and good permeability. The electrospinning nanofiber framework can effectively

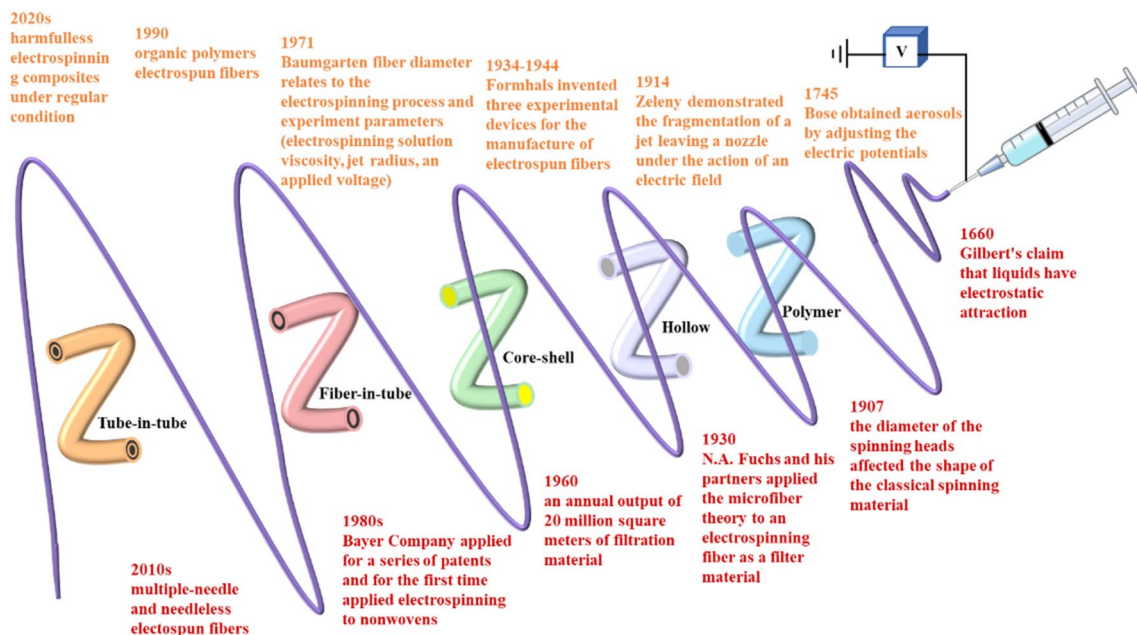


Fig. 1 Development of electrospinning briefly

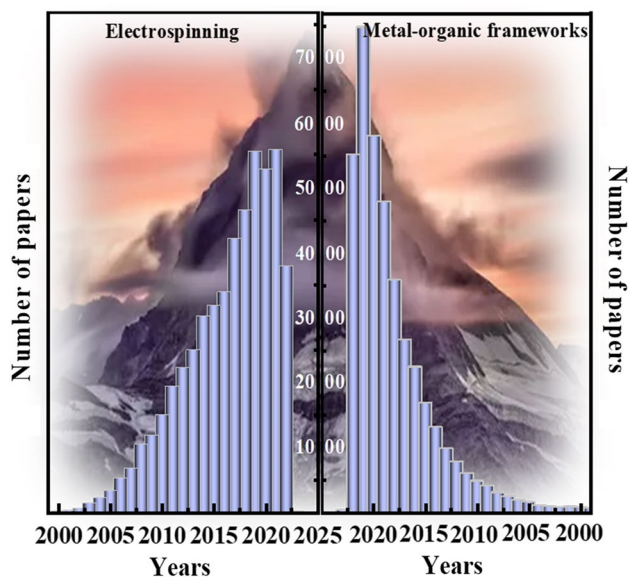


Fig. 2 Number of published papers between 1998 and 2022.10, with the keyword “electrospinning and metal–organic frameworks”

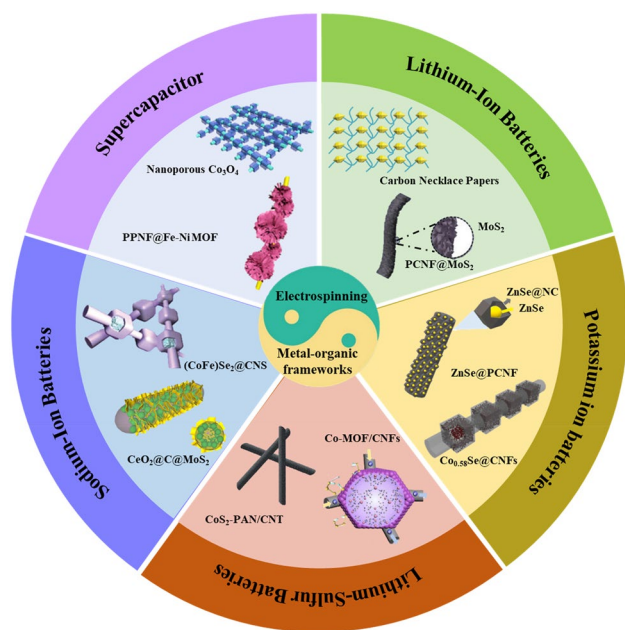


Fig. 3 Schematic diagram of the main application fields of MOF nanofibers

inhibit the agglomeration of MOF particles and increase the utilization of active sites.

In this paper, the latest research results of MOFs nanofiber composites materials and their derived composites materials are reviewed and applied to supercapacitors, lithium-ion batteries, sodium-ion batteries, potassium-ion batteries, and lithium–sulfur batteries (Fig. 3). It highlights

that the structural design has a great influence on the electrochemical performance. The development prospects and challenges of MOF nanofibers have prospected. This provides more references for subsequent researchers in electrode design [92–95].

Feasible Strategies and Preparation of MOF-Based Materials

Electrospinning is a way of making composite nanofiber membranes from polymers and MOFs. Under the action of high-voltage static electricity, different kinds of polymers and different solvents can form a specific electrospinning solution. There are usually two ways to prepare the MOF/polymer fiber membrane via electrospinning: direct electrospinning of the prepared MOFs and polymers; in situ growth of MOFs on the surface polymers nanofiber by electrospinning [96–98].

Structural Design MOFs’ Hybrid

MOFs’ powder materials are usually synthesized first. As long as the selected MOF does not react with the electrospinning solution, the original channel and structure of the MOFs material will not be damaged during the electrospinning process. Subsequently, parameters (the concentration of MOFs, applied voltage, the viscosity of the slurry, injector of diameter, and type of needle) could be adjusted to optimize the experimental conditions. This process enables MOFs to be directly embedded into the polymer nanofiber. Finally, a large number of MOFs polymer nanofibers with controllable structures are as-obtained [99, 100].

In Fig. 4a, Lu’s group prepared the membranes of UIO-66/PVA composite by rapid electrospinning technique [101]. PVA contained a hydroxyl group and the MOF contains carboxylic acid, which is converted to an ester bond through esterification, making MOF and PVA connected to form the fibrous network. The liquid electrolyte immersed into the electrospun MOF–PVA composite membranes (EMP). The anions of the electrolyte automatically adsorbed to the MOF and fixed in the MOF channels.

This process improved the efficient transport of lithium ions in the electrolyte, increased the Li-ion migration number and lithium-ion conductivity. In addition, the introduction of MOF particles reduced the decomposition of the electrolyte and promoted the electrode reaction kinetics (Fig. 4b). Figure 4c displays an SEM of EMP. The overall morphology was beaded fibrous, and the regular octahedron shape of the MOF distributed in the PVA nanofiber. Yin et al. produced ZIF-7/PAN nanofiber with the variation of the slurry fabrication process electrospinning (Fig. 4d). In this process, the raw materials of ZIF-7 directly put into

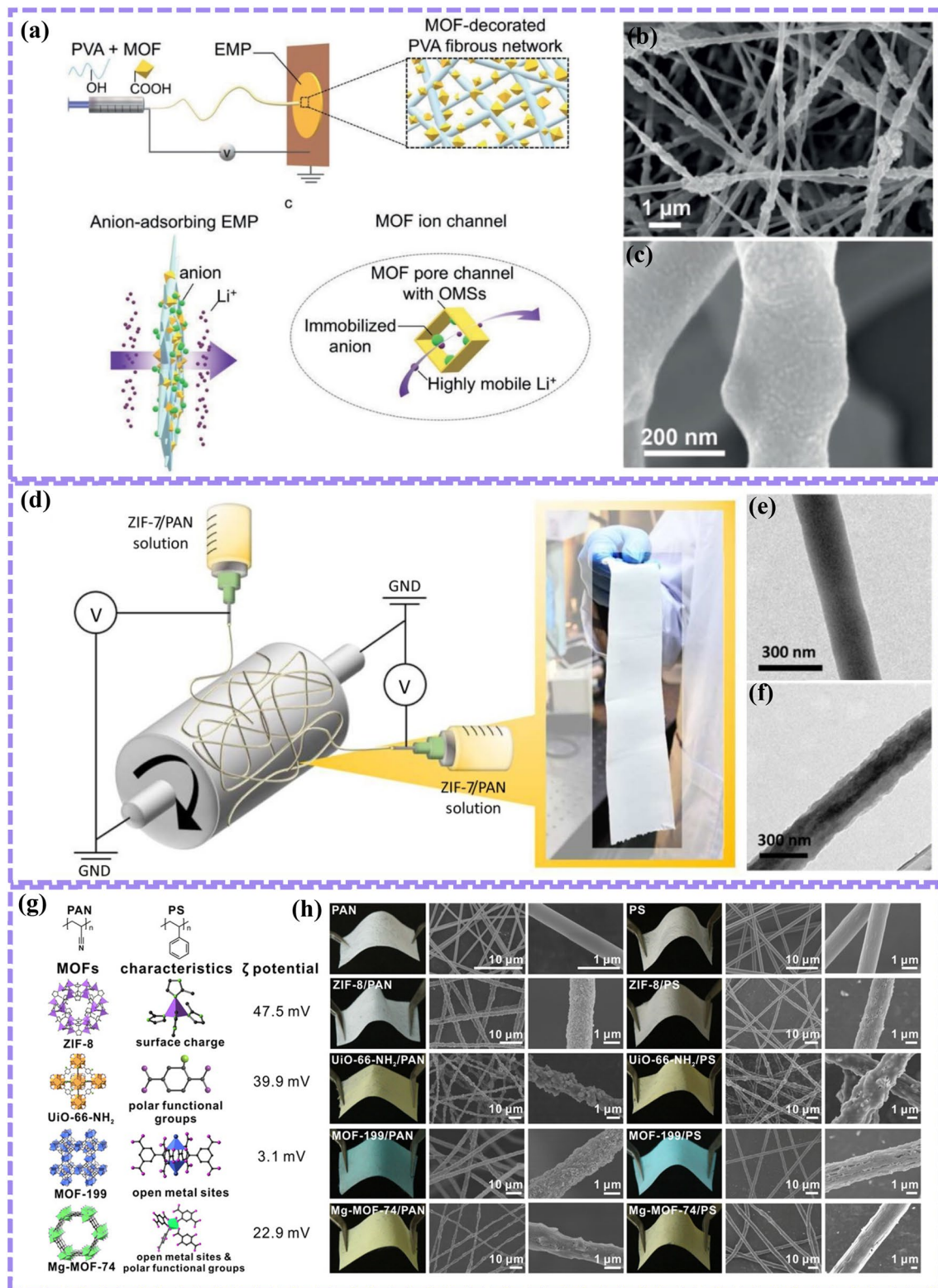


Fig. 4 Schematic diagram of MOF directly added into the electrostatic spinning to prepare materials. **a** MOF–PVA composite membrane; **b–c** the SEM of MOF–PVA; reprinted with permission from ref. [101], Copyright 2019, Wiley-VC; **d** ZIF-7/PAN; **e** TEM images of PAN-NF; **f** ZIF-7/PAN-NF; reprinted with permis-

sion from ref. [102], Copyright 2016, Wiley-VC; **g** the structure of different types of MOFs; **h** optical and scanning electron microscopy of composite materials; reprinted with permission from ref. [103], Copyright 2016, American Chemical Society

the electrospinning solution. This method helped to control the size of the ZIF-7 much less than the diameter of the PAN nanofibers. In Fig. 4e, f, the TEM of a single PAN nanofiber owned a slippy surface and a uniform diameter of 200–300 nm. The ZIF-7/PAN composite demonstrated that ZIF-7 evenly was distributed in the fibers, and the fiber surface became more corrugated [102]. Wang and his team prepared a series of flexible composite nanofiber films by embedding four MOFs into three polymers (PAN, PVP, and PS) by electrospinning (Fig. 4g).

The composite membrane was used as a contaminant filter. Agglomeration was prevented by adjusting the optimal loading between the MOFs and the polymer. Pollutants interact with MOFs in different forms to achieve filtration. Figure 4g shows that the four MOFs have a unique spatial structure that can effectively adsorb different functional groups, enhancing the ability of the composites to capture different types of pollutants in air filters. Figure 4h shows the digital photos and corresponding SEM photos of different MOF on different electrospinning substrates [103]. Different Ni-BDC loadings of Ni-BDC/PAN nanofiber membranes were obtained, and the proton conduction property of the composite was studied by Liu's group. The imidazole molecules added into one-dimensional MOF/polymer fibers significantly affected their proton conductivity. The Ni-BDC and imidazole put into the electrospinning solution to fabricate the composite film [104]. The structure of Ni-BDC promoted the movement of imidazole molecules.

Hybrids of MOF-Derived Nanostructures

MOF derivatives are mainly divided into porous carbon and composite materials. It has the following advantages in energy storage. Hollow and porous structures contribute abundant active sites; multi-dimensional derivative materials could provide more ways of electron transport; the derivative film materials can play their flexible and self-supporting characteristics. Therefore, researchers have made some achievements in MOF-derived materials in recent years [105–109].

The remarkable surface area, lightweight, super-long stability, and open porosity of carbon materials have been diffusely applied in $\text{Li}^+/\text{Na}^+/\text{K}^+$ ion batteries and supercapacitors (SCs) [110–115]. At the same time, electrospun nanofiber materials form a series of carbon-based composites through annealing treatment, which has also become a hotspot of supercapacitor materials. Kim et al. designed the flexible membrane (Co/N-CNT@PCNF900) via a facile method, which processed no need for extra reducing gases [116]. $\text{Co}(\text{NO}_3)_2$ @PAN-NF membrane formed by adding $\text{Co}(\text{NO}_3)_2$ to polyacrylonitrile (PAN) by electrospinning. The as-prepared membrane put into a

2-methylimidazole solution and obtained ZIF-67@PAN-NF, which subsequently annealed to obtain Co/N-CNT@PCNF900 in Fig. 5a. The SEM of Co/N-CNT@PCNF900 nanofibers had an entwined N-CNT network structure, which was beneficial to increase the flexibility of the membrane. The characteristics of the flexible and porous carbon nanofibrous (Co/N-CNT@PCNF900 membrane) possessed uniform pore size distribution, and homogeneous metal atoms, which displayed remarkable electrocatalysis and SCs. The design strategy combined the advantages of MOF and electrospinning to form a low-cost and universal method. Sun reported a kind of nitrogen-doped nanofiber carbon (N-NFC) derived from MOF in Fig. 5b. MOF layers grew on the electrospun polymer nanofiber with controllable size and uniform morphology. The ions between polar groups on the polymer side chain and the metal promoted nucleation of MOF, and steric hindrance resulted in uniform growth of the MOF. After high-temperature annealing, these nanofibers transformed into N-NFC. The amount of the outer carbon shell could be regulated by the ratio between organic ligands and metal ions. A low concentration of an organic ligand could increase the size of ZIF-8, which also reduced the amount of ZIF-8 on the surface. N-NFC-8 exhibited the best concentration ratio, and the hollow carbon skeleton was evenly distributed on the surface [117]. The core-sheath nanofibers transformed into N-NFC during high-temperature pyrolysis. N-NFC structure has the following advantages: (1) The highly conductive one-dimensional nanofiber structure is the core; (2) the outer layer is a uniformly distributed hollow carbon shell; (3) there are a large number of micro/mesoporous pores in the structure; (4) uniform n-doping is achieved. Finally, it shows outstanding electrochemical performance.

Recent Progress of MOF-Based Materials in Energy Storage

For the past few years, supercapacitors, lithium/sodium-ion batteries, play a significant role in energy storage [118–121]. The choice of electrode materials determine its electrochemical performance. Therefore, a great deal of researches have focused on exploring electrode materials with high efficiency, long cycle life, low cost, and high specific capacitance. However, MOF nanofibers contribute more electrochemistry active sites in the reaction, due to their aperture structure with larger surface area and adjustable aperture. In this section, research on MOF nanofibers and their derived materials progress and summarize their energy storage performance in Table 1.

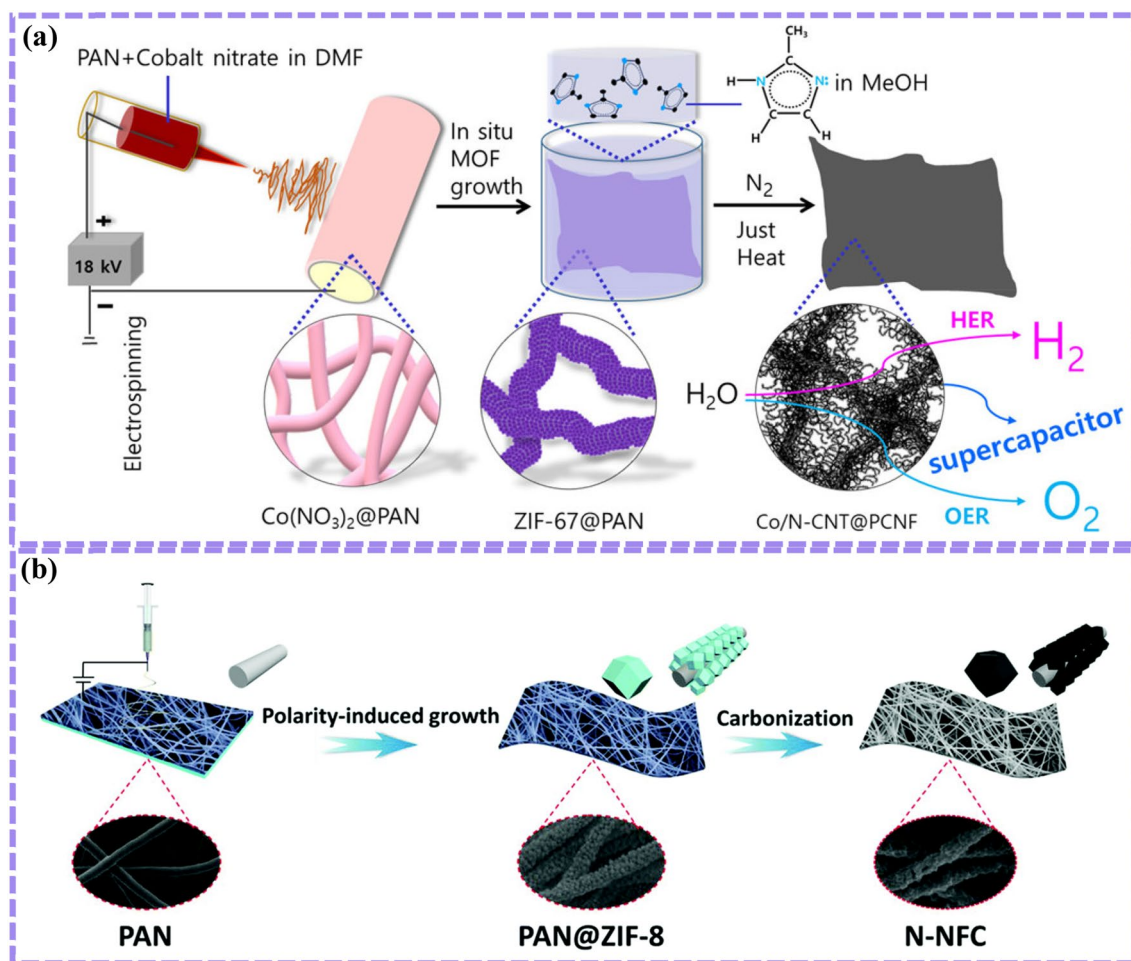


Fig. 5 Preparation mechanism of MOF-derived carbon composites. **a** Co/N-CNT@PCNF membrane; reprinted with permission from ref. [116], Copyright 2021, American Chemical Society; **b** nitrogen-

doped Nanocarbon (N-NFC); reprinted with permission from ref. [117], Copyright 2019, Royal Society of Chemistry

Supercapacitors

The supercapacitor is a kind of energy storage device that can carry out high-power fast charging (within a few seconds) and ultralong cycle life. MOFs and their derived materials tend to have a large active surface area, reasonable pore size, and chemical stability. At the same time, the metal ions contained in MOFs can also provide more sites for pseudocapacitor energy storage. Therefore, MOF nanofibers and derived materials have attracted wide attention in the application of supercapacitors.

Wang demonstrated a simple strategy to prepare bimetallic MOFs on preoxidized polyacrylonitrile nanofibers (PPNFs). The metal ions in the structure provided pseudocapacitor energy storage for electrochemical reactions. First, polyacrylonitrile was used as a raw material to form fiber films by electrospinning and calcination to obtain PPNFs. Then, through solvothermal reactions, metal ions coordinated with terephthalic acid to obtain the M-Ni MOF in

Fig. 6a [122]. In Fig. 6b, c, the SEM images of PPNF@Co–Ni MOF, and PPNFs are completely covered by a globular Co–Ni MOF with a diameter of 1.4–1.8 μm . However, when Zn ions are introduced, Zn–Ni MOF grew evenly on PPNFs, but the flower globules disappeared, and the surface of PPNFs was relatively smooth with only a few nanosheets. Meanwhile, the hierarchical flower-like nanosheets demonstrated a remarkable specific surface area. The introduction of Co into PPNF@Ni MOF improved redox activity, increased electronic conductivity, and exhibited the synergistic effect of different elements. Among them, PPNF@Co–Ni MOF showed remarkable electrochemical performance in supercapacitors. At the current density of 1 A g^{-1} , the specific capacity delivered 1096.2 F g^{-1} (548.1 C g^{-1}). Yoon reported an easily prepared and low-cost Mn@ZnO/CNF electrode material for supercapacitors, as shown in Fig. 6d [123]. Mn-doped ZIF-8 directly grown on polyacrylonitrile nanofibers. The composite fiber carbonized to form a dodecahedron Mn@ZnO with CNF as the core and

Table 1 The MOF nanofiber and derived-MOFs' materials for energy storage performance

MOF	Final nanofibers	Route	Application	Performance	References
Mn-BTC	ysMnO _x @NC	Direct electrospinning	Lithium-ion battery	880 mA h g ⁻¹ at 0.1 A g ⁻¹	[106]
Ni-CAT	CNF@Ni-CAT	Surface in situ growth	Supercapacitor	502.95 F g ⁻¹ at 0.5 A g ⁻¹	[116]
ZIF-8	Nitrogen-doped nanofibrous carbon	Surface in situ growth	Supercapacitor	387.3 F g ⁻¹ at 1 A g ⁻¹	[117]
Co–Ni MOF	PPNF@Co–Ni MOF	Surface in situ growth	Supercapacitor	1096.2 F g ⁻¹ at 1 A g ⁻¹	[122]
ZIF-8	Mn@ZnO/CNFs	Surface in situ growth	Supercapacitor	501 F g ⁻¹ at 1 A g ⁻¹	[123]
ZIF-67	Nanoporous Co ₃ O ₄	Direct electrospinning	Supercapacitor	970 F g ⁻¹ at 1 A g ⁻¹	[129]
ZIF-67	CNT@HCNF	Surface in situ growth	Supercapacitor	712 F g ⁻¹ at 1 A g ⁻¹	[130]
ZIF-8	PCNF@MoS ₂	Direct electrospinning	Lithium-ion battery	1116.2 mA h g ⁻¹ at 1 A g ⁻¹	[137]
ZIF-67	Carbon necklace paper	Direct electrospinning	Lithium-ion battery	1200 mA h g ⁻¹ at 0.2 A g ⁻¹	[138]
ZIF-67	CoSn _x	Direct electrospinning	Lithium-ion battery	657.7 mA h g ⁻¹ at 0.1 A g ⁻¹	[140]
ZIF-67	SnO ₂ -Co ₃ O ₄	Direct electrospinning	Lithium-ion battery	1287 mA h g ⁻¹ at 0.5 A g ⁻¹	[142]
ZIF-67	ZIF-67/CNFs	Surface in situ growth	Lithium–sulfur battery	1334 mAh g ⁻¹ at 1 C	[38]
ZIF-8	MoS ₂ @N-CNFs	Direct electrospinning	Lithium–sulfur battery	920 mAh g ⁻¹ at 0.2 C	[143]
ZIF-67	CoS ₂ -SPAN-CNT	Surface in situ growth	Lithium–sulfur battery	1,240 mAh g ⁻¹ at 0.2 C	[144]
Cu-BTC	Cu-BTC modified PMIA	Direct electrospinning	Lithium–sulfur battery	1272.2 mAh g ⁻¹ at 0.5 C	[145]
ZIF-67	(CoFe)Se ₂ @CNS	Direct electrospinning	Sodium-ion battery	262.9 mA h g ⁻¹ at 0.1 A g ⁻¹	[151]
Ni/Co-MOF	NiCo ₂ O ₄ /NiO/carbon nanofibers	Surface in situ growth	Sodium-ion battery	210 mA h g ⁻¹ at 0.1 A g ⁻¹	[154]
MIL-88A-Fe	Fe ₇ S ₈ /N-CNFs	Direct electrospinning	Sodium-ion battery	649.9 mAh g ⁻¹ at 0.2 A g ⁻¹	[155]
ZIF-67	CNT@CoSSe@C	Surface in situ growth	Sodium-ion battery	479.4 mA h g ⁻¹ at 1 A g ⁻¹	[156]
ZIF-67	Co _{0.85} Se@CNFs	Direct electrospinning	Potassium-ion battery	353 mAh g ⁻¹ at 0.2 A g ⁻¹	[157]
ZIF-8	ZnSe@PCNF	Direct electrospinning	Potassium-ion battery	270 mA h g ⁻¹ at 0.5 A g ⁻¹	[158]
ZIF-8	MoP@NPCNFs	Direct electrospinning	Potassium-ion battery	320 mA h g ⁻¹ at 0.1 A g ⁻¹	[159]

a high surface area. Heat treatment carbonization of MOFs allowed the metal oxides to be well-distributed on the porous carbon framework. This structure provided more pathways for fleetly electron transfer and increased the active site of the Faraday reaction. Meanwhile, the introduction of carbon material increased the electroconductivity of the composite [124–128]. The SEM of Mn-ZnO showed the uniform growth of dodecahedron on the surface of polyacrylonitrile fiber (Fig. 6e) and the optical photo of flexibility supercapacitor devices, as shown in Fig. 6f.

Xu's group prepared the 3D macrostructures' construction of nanoporous Co₃O₄, which was synthesized by the PAN/ZIF-67 nanofibers after annealing treatment in Fig. 7a. Co₃O₄ derived in situ from MOF and distributed uniformly in electrospun polyacrylonitrile nanofibers. After calcination, Co₃O₄ inherited the 3D pore structure from the PAN/ZIF-67 nanofibers. The 3D network increased the diffusion path of ions. The unique spatial structure and appropriate porosity enhanced the enhancing capacitance. The high capacitance of the Co₃O₄ electrode exhibits 970 F g⁻¹ at 1 A g⁻¹ [129]. Similarly, in 2021, Kim and his team used similar nanoparticles infused with tiny Co₃O₄ (NPs) [130]. After annealing, electrospinning PAN became the CNFs. Cobalt carbonate hydroxide nanohairs grown on CNFs by hydrothermal method and completely transformed into ZIF-67@CNFs. Under low temperatures and no reducing atmosphere,

a 3D array Co₃O₄/N-CNTs@CNF is obtained. This design enabled MOF as template not only to serve as the source of CNTs, N-doping, and a small amount of Co₃O₄ NPs, but also to ensure a large specific surface area, high porosity, and uniform composition distribution in the composite structure. The multi-step structure construction and annealing were beneficial to the stability of the three-dimensional structure. In this design idea, through low temperature and non-reducing gas, and without the need for additives could design a composite structure with multiple components.

Han reported the core-shell structure of CNF@Ni-CAT as a flexible membrane by electrospinning [114]. After the carbonization of 800 °C, the electrospinning of PAN converted to carbon nanofibers (CNFs). Ni-CAT nanorods grown on the surface to accelerate the transport between ions (Fig. 7b). This design strategy effectively improved the agglomeration problem of MOFs and increased the contact area between the electrode material and the electrolyte. The composite film material also had excellent flexibility, which made a certain contribution to the application of flexible electronic energy storage. Kim's group prepared highly porous N-doped carbon nanotubes (N-CNTs) on hollow carbon nanofibers, owing to a high capacitance, as shown in Fig. 7c [131]. First, polyacrylonitrile (PAN) and polymethyl methacrylate (PMMA) electrospun to obtain the sheath-core nanofibers. Then,

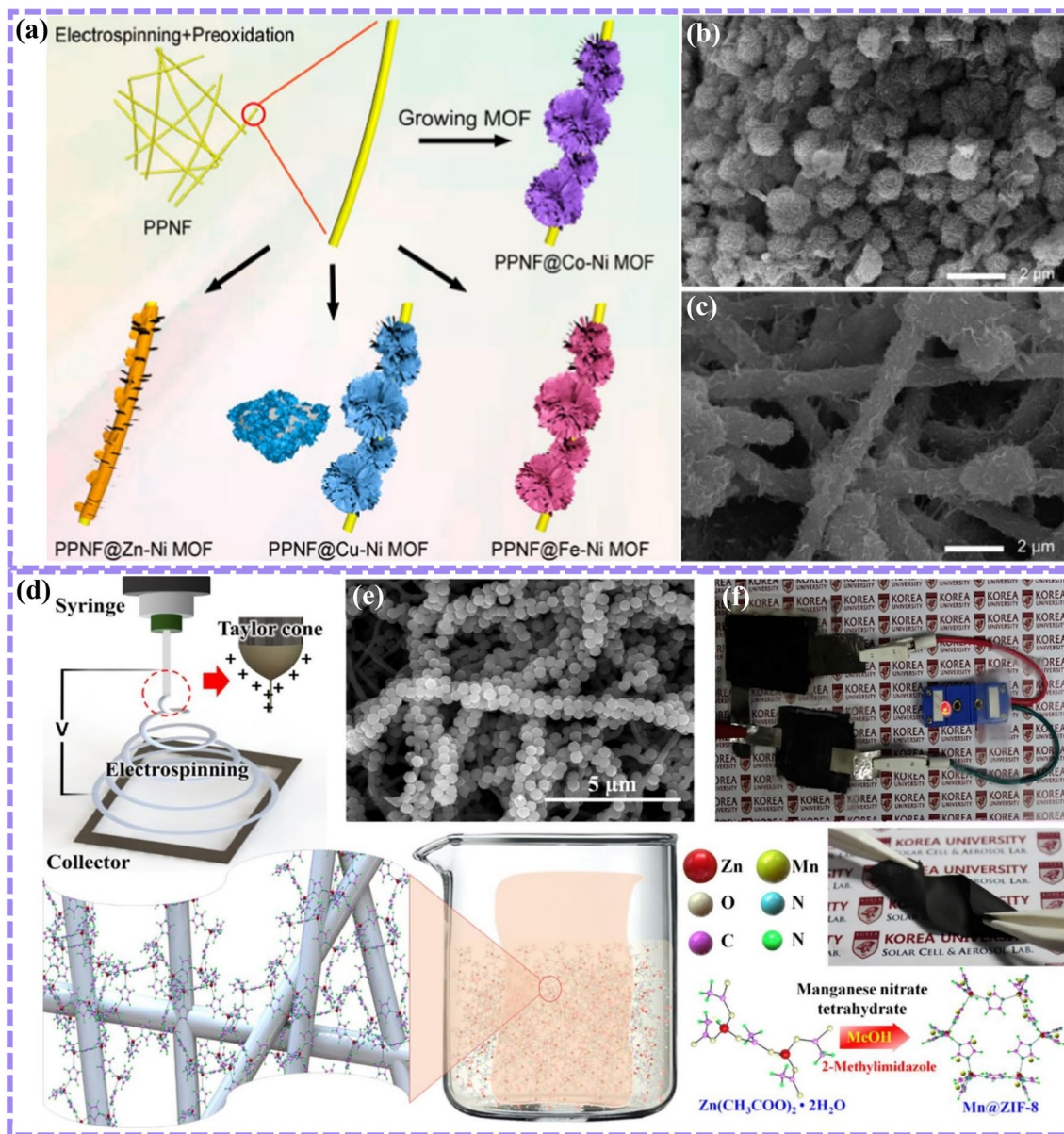


Fig. 6 Fabrication diagram of annealed electrospinning composite film electrode in supercapacitor. **a** M-Ni-MOF (M=Co, Zn, Cu, and Fe); **b** SEM of as-obtained materials PPNF@Co-Ni-MOF; **c** PPNF@Zn-Ni-MOF; MOF; reprinted with permission from ref. [122], Copyright 2020, American Chemical Society; **d** Mn@ZnO/CNFs; **e** SEM of Mn@ZnO/CNFs; **f** flexible electrode LED power supply; reprinted with permission from ref. [123], Copyright 2019, Elsevier

the ZIF-67 grew evenly on the sheath–core nanofibers. The ZIF-67/sheath–core nanofibers were converted into hollow carbon nanofiber composite porous N-doped carbon tubes (CNT@HCNF-1.5) by the one-step method under an optimal precursor ratio and appropriate heat treatment temperature. The preparation processes were simple and did not require reducing gas. CNT@HCNF-1.5 reached a capacitance approaching 712 F g⁻¹.

Lithium-Ion Batteries

Lithium-ion batteries (LIBs) are the core component of traditional storage devices and electric vehicles because of their ultra-high energy density and admirable cycle life. However, LIBs still face many challenges. For example, in the process of Li-ion intercalation/deintercalation, the volume of the electrode material changes, resulting in capacity

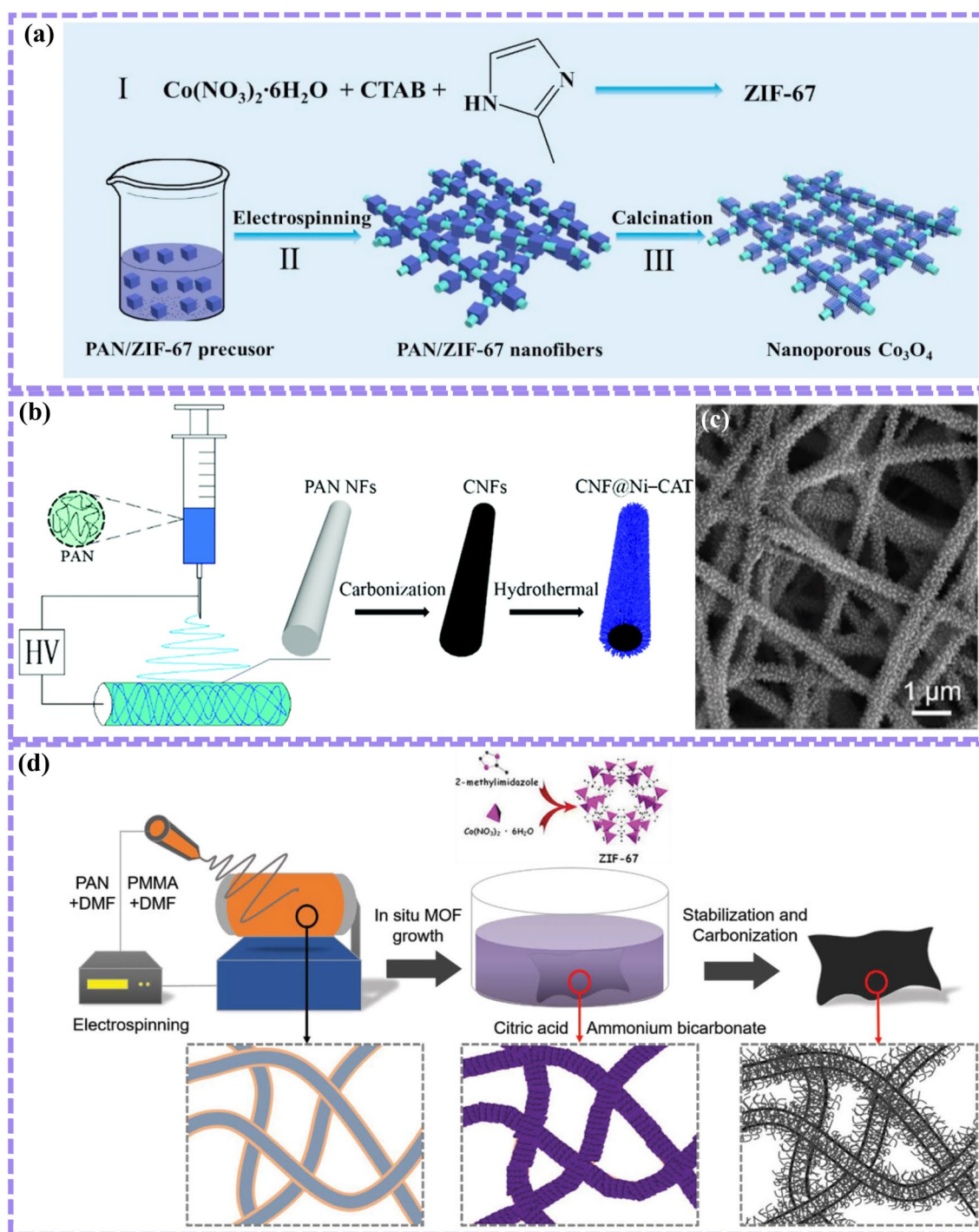


Fig. 7 Preparation process of MOF-derived nanostructures in supercapacitor. **a** Design idea of nanoporous Co_3O_4 ; reprinted with permission from ref. [129], Copyright 2021, Elsevier, **b** CNF@Ni-CAT;

reprinted with permission from ref. [114], Copyright 2019, Royal Society of Chemistry; **c** CNT@HCNF-x electrode; reprinted with permission from ref. [131], Copyright 2022, Wiley-VC

attenuation; ion diffusion and transport are slow in some electrode materials. Therefore, it is very important to design electrode materials carefully for lithium-ion energy storage. The porous structure of MOF and its derivatives buffered the volume change during the process of lithium/dilithium

and improve cyclic stability. The integrated electrode design avoids using a binder and improves the overall conductivity of the electrode material [132–136].

Zhang and their partners proposed that MoS_2 nanoplates were directly grown on the surfaces of N-doped porous

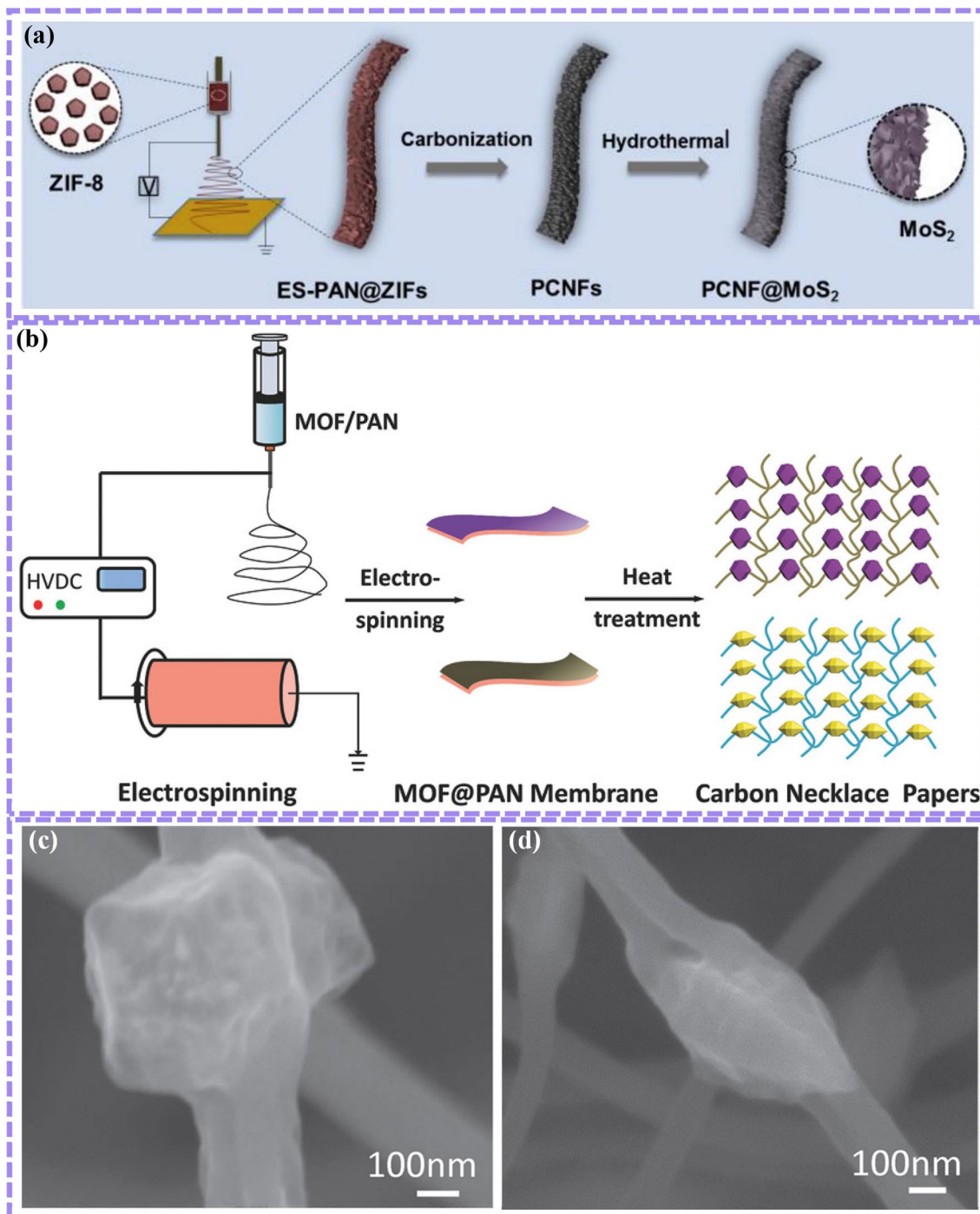


Fig. 8 The scheme for the MOF-derived carbon fiber preparation diagram in lithium-ion battery. **a** PCNF@MoS₂; reprinted with permission from ref. [137], Copyright 2019, Elsevier; **b** carbon necklace

paper; SEM of derived from **c** MIL-88@PAN and **d** ZIF-67@PAN; reprinted with permission from ref. [138], Copyright 2017, Wiley-VC

carbon nanofibers (PCNFs) and obtained hierarchically from PCNF@MoS₂ fibers by electrospinning. Figure 8a shows the synthesis process of PCNF@MoS₂. High-length-diameter nanofibers of ES-PAN@ZIFs were prepared using PAN and nitrogen-rich ZIF-8 NPs by electrospinning. ES-PAN@ZIFs

nanofibers annealed in an Ar atmosphere to get N-doped PCNF. By hydrothermal method, homogeneous MoS₂ grown on the PCNFs. The well-designed PCNF@MoS₂ could prevent Li⁺ from damaging the material structure and good reversibility. The capacity at 1 A g⁻¹ current density was

1116.2 mAh g⁻¹ after 450 cycles [137]. Zhang and his partners proposed an MOF-derived carbon necklace structure, which interconnected by heteroatoms and metal nanoparticles [138]. ZIF-67 and MIL-88 severally put into polyacrylonitrile (PAN) electrospinning solution to form MOF@PAN chain precursor films by electrostatic spinning, as shown in Fig. 8b. ZIF-67@PAN and MIL-88@PAN derived carbon necklace paper (CNPs) and indicated as ZCNP and MCNP by direct pyrolyzation of precursor film in the N₂ atmosphere. During the pyrolysis process, the MOFs transformed into nitrogen-doped porous carbon materials, metal particles, which facilitated the storage of lithium ions. PAN fibers pyrolyzed to form a 3D conductive network, which formed a larger contact area, thus promoting the fast transfer of electrons in the electrochemical reaction. Meanwhile, this material had a self-supporting structure, which regarded as an anode of LIBs for performance testing without additional conductive agents and binders. The ZCNP and MCNP exhibited outstanding cyclic life and an impressive capacity of 1200 and 980 mAh g⁻¹ in the current density of 200 mA g⁻¹. Figure 8c shows the SEM of the ZIF-67-derived structure. After heat treatment, polyhedral nanocages embedded into the 3D carbon fiber conductive network. ZIF-67 could still maintain its polyhedral structure. The wrinkles on the surface of polyhedra related to the decomposition of organic groups in MOF and PAN. It displayed similar results derived from MIL-88@PAN in Fig. 8d. Tang et al. introduced 7 nm Mn₃O₄ into MOF-derived nitrogen-doped porous carbon fibers (NPCFs) via the sol–gel method and electrostatic spinning method [139]. The design idea was beneficial to reduce the agglomeration of Mn₃O₄ in composites. The open space structure can relieve the volume expansion during Li⁺ charge/discharge cycles. Rugged one-dimensional construction contributed to outstanding electrical conductivity. NPCFs provided a more effective path for rapid ion and electron transfer. The strongly coupled interaction between Mn₃O₄ and NPCFs occurs, and its electrochemical property was observably enhanced. The Mn₃O₄/NPCFS-1.4 flexible material can reach 1058 mAh g⁻¹ at 50 mA g⁻¹.

Zhang's group reported an assisted anion-exchange strategy for CoSnx@CPAN nanofibers, by coaxial electrospinning in Fig. 9a. Co(CH₃COOH)₂ and 2-methylimidazole stirred separately in a PAN solution. The two solutions transferred into two identical syringes through coaxial electrostatic spinning, and ZIF-67@PAN nanofiber membranes were formed. The composite nanofibers immersed in Na₂SnO₃ solution for anion exchange. Anion exchange required neither additional input of energy nor a complex experimental environment. This special design concept encapsulated well-dispersed nanoparticles in a three-dimensional hierarchy polymer nanofiber frame. CoSnx@CPAN enhanced the storage and diffusion of electrons/charges. The obtained CoSnx@CPAN and CoSn(OH)₆@

PAN showed remarkable performance in lithium-ion batteries [140]. Liang et al. presented a process via electrospinning Mn-MOF. After annealing, the yolk–shell MnOx contained carbon nanofibers in Fig. 9b [106]. As shown in Fig. 9c, Mn-BTC spheres and polyacrylonitrile (PAN) formed a fiber composite material with strings of beads using an electrostatic spinning structure. Increasing the concentration of Mn-BTC electrospinning solution can increase the number of spheres in the fiber composite. Subsequently, the Mn-BTC@PAN composite material was peroxidation treated in the air at 300 °C. The sieve shell structure of the Mn-BTC nanospheres was oxidized in the pre-oxidation step and showed in the TEM of Fig. 9d. Finally, it is further flamed in N₂ at 600 °C for 2 h to form ysMnOx@NC nanofibers (Fig. 9e). The intermediate heating step can stabilize the structure of the nanofibers and facilitate the retention of the structure after carbonization. The yolk–shell of MnOx accepted volume expansion in lithium-ion migration processes and effectively prevented the pulverization of active substances, while the outer carbon fiber shell ensured the integrity of the structure during charge/discharge. The morphology and composition of yolk–shell MnOx composite nanofibers with different loading loads investigated and characterized. It proposed that the preparation mechanism of this structure might be Oswald curing and the Kirkendall process. After 1000 cycles, this structure still displayed excellent stability. The dual-buffer design can also present the process of lithium/dilithium by ex situ imaging. This synthesis strategy had certain versatility and can be used as a reference for preparing other transition metal oxides [141]. Kim et al. prepared SnO₂–Co₃O₄ nanofibers with oxygen vacancies, as shown in Fig. 9f. ZIF-67, Sn precursor, and PVP mixed as an electrospinning solution for electrospinning. ZIF-67 uniformly distributed on the surface of PVP fiber. After calcination, ZIF-67 decomposed on the nanofibers to form the mesoporous site SnO₂–Co₃O₄. Due to the introduction of ZIF-67, more oxygen vacancies formed as active sites for lithium storage, which improved the conductivity of the composites and facilitated the transport of ions and electrons. In addition, one-dimensional structures with high surface area and high porosity can show excellent electrochemical performance, with a reversible capacity of up to 1287 mA h⁻¹ at the current density of 500 mA g⁻¹, after 300 cycles [142].

Lithium–Sulfur Batteries

Lithium–sulfur battery demonstrates potential in the electrochemical application, owing to its advantages of splendid theoretical energy density (2600 Wh kg⁻¹), low cost, and sufficient reserve. Unfortunately, the rapid dissolution of polysulfide results in decrease its capacity and cycle life. The key to solving those problems is to design effective

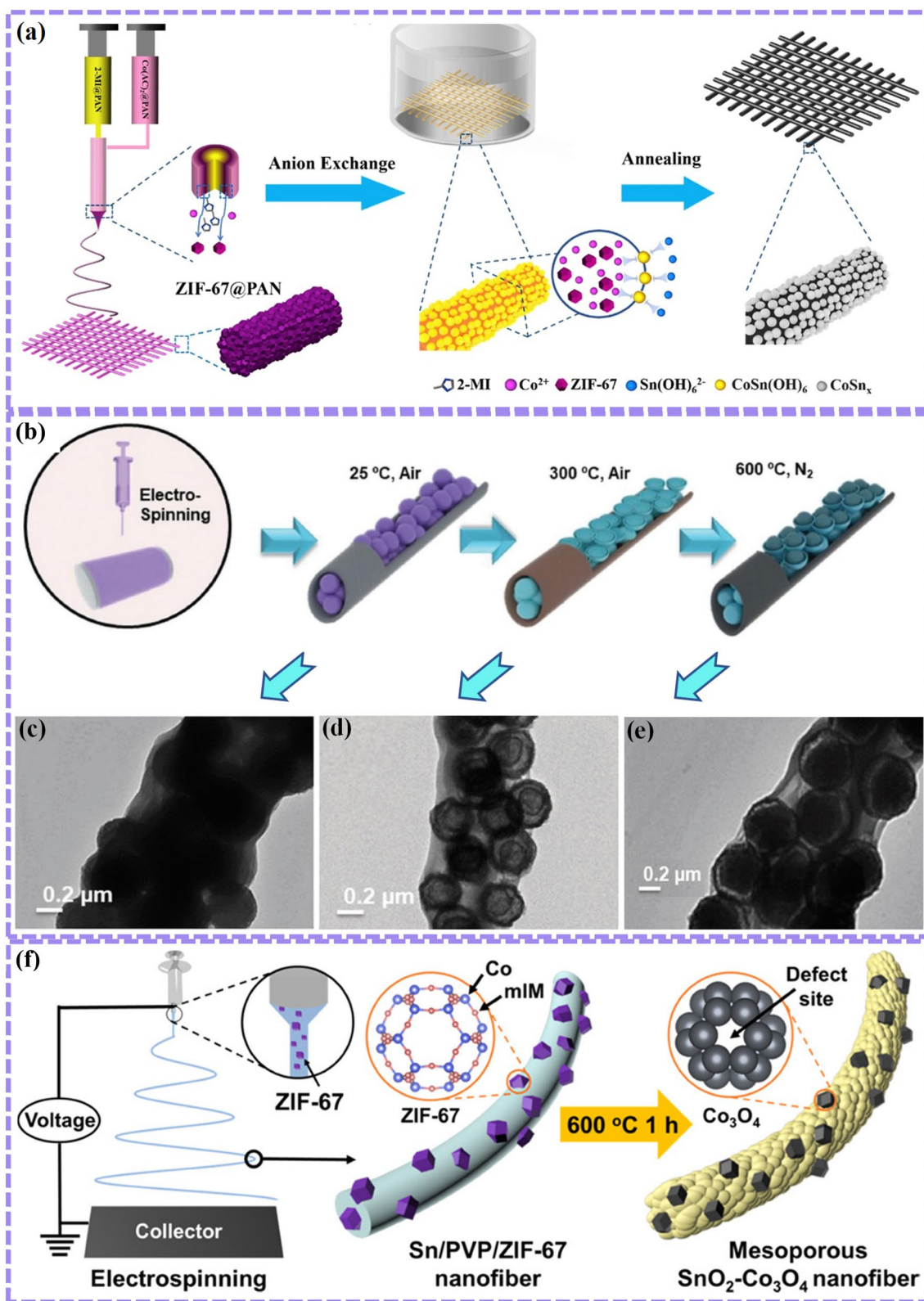


Fig. 9 Schematic diagram of MOF-derived composite fiber membrane in lithium-ion batteries. **a** CoSn_x nanoparticles; reprinted with permission from ref. [140], Copyright 2020, Elsevier; **b** $\text{ysMnO}_x\text{@NC}$; the TEM image of **c** Mn-BTC@PAN-2. **d** Pre-oxidized Mn-

BTC@PAN-2; **e** $\text{ysMnO}_x\text{@NC}$ -2; reprinted with permission from ref. [106], Copyright 2019, Wiley-VC; **f** Mesoporous $\text{SnO}_2\text{-Co}_3\text{O}_4$ nanofibers; reprinted with permission from ref. [142], Copyright 2018, American Chemical Society

structures to prevent dissolution. One feasible way to overcome the above shortcomings is to construct electrode materials with high conductivity and abundant porosity. MOF-derived fiber electrodes offer great potential in this regard.

Qiu and his partners designed ZIF-67 as a functional sandwich structure grown on carbon nanofibers (CNFs). The structure had a uniform microporous carbon skeleton and mesoporous ZIF-67 as the active site, which can effectively adsorb polysulfide and accelerate the movement of polysulfide. At the same time, the carbon nanofibers' structure can promote the electroconductibility of the ZIF-67/CNFs' material and supply a pathway for electron transfer, as shown in Fig. 10a. Therefore, a well-designed sandwich

structure helped to inhibit the dissolution of polysulfide and reduce the shuttle effect utilizing physical blockade. Finally, the ZIF/CNFs displayed 1334 mAh g^{-1} and excellent cyclic life in 1 C. [38]. Yao et al. presented the 3D ivy-structured MoS_2 @N-CNFs via electrospinning. First, N-CNFs films obtained by electrospinning and annealing of PAN and ZIF8, and then, MoS_2 nanosheets uniformly grown on the surface of N-CNFs fibers by the hydrothermal method in Fig. 10b [143]. The MoS_2 @N-CNFs composite membrane could be directly used as a cathode for lithium/polysulfide batteries. N-CNFs films with high conductivity can effectively reduce the internal resistance of the electrode as a lithium polysulfide. Meanwhile, the

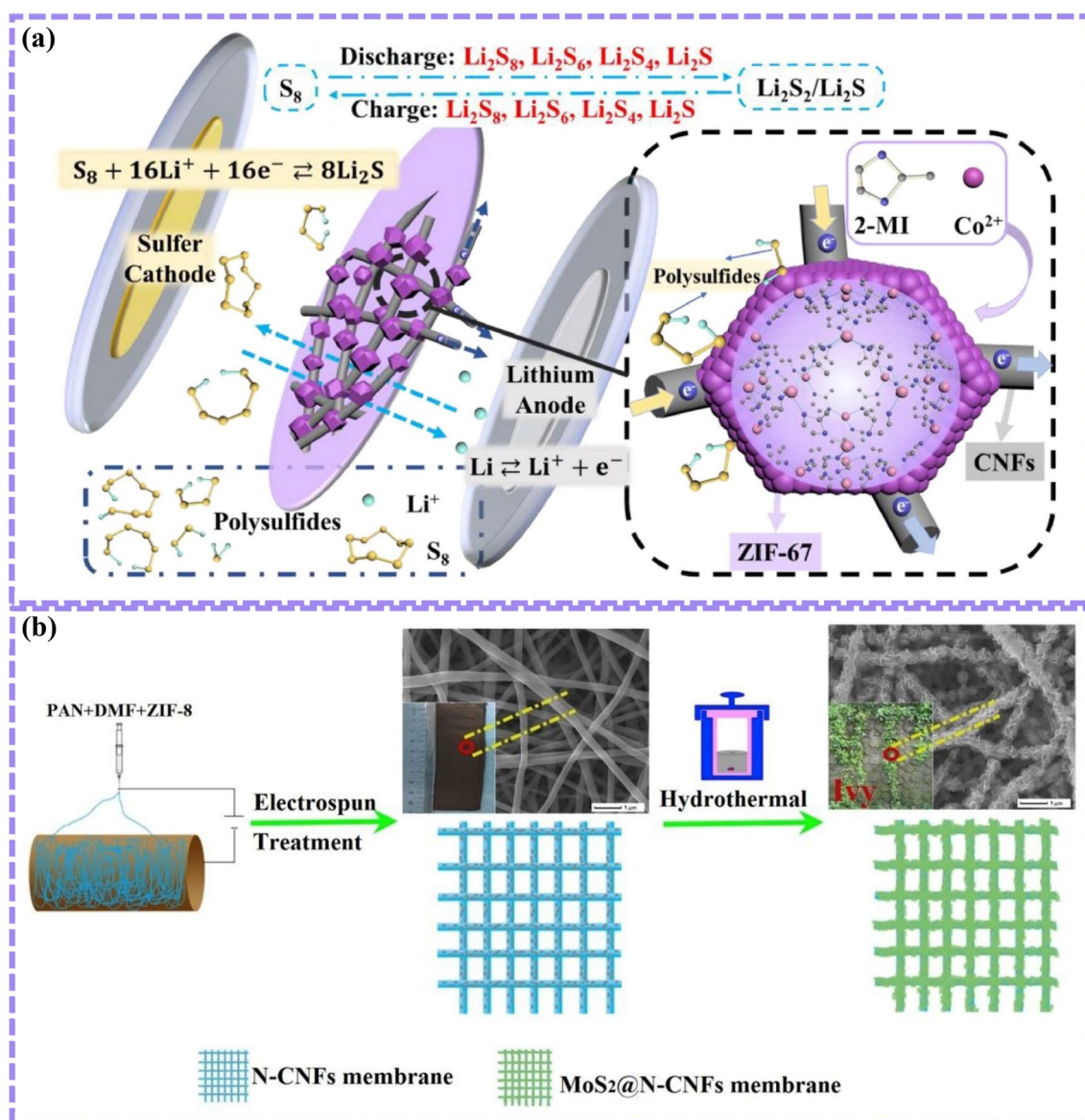


Fig. 10 Schematic illustration of the as-obtained in the lithium-sulfur battery. **a** ZIF-67/CNFs; reprinted with permission from ref. [38], Copyright 2021, Elsevier; **b** MoS_2 @N-CNFs; reprinted with permission from ref. [143], Copyright 2019, Elsevier

MoS₂ nanosheet chemically combined with the collector. It had a high theoretical capacity and strong binding energy with polysulfide. The pyridine nitrogen mesopores in N-CNFs could be used to fix dissolved lithium to form polysulfide. The MoS₂@N-CNFs cathode demonstrated a discharge capacity of 920.0 mAh g⁻¹ at 0.2 C. DFT calculation showed that MoS₂ nanosheet sulfide/metal–oxide nanosheet composite N-CNFs were a feasible strategy to promote the electrochemical behavior of lithium–sulfur batteries anode.

Deng et al. fabricated high sulfur load CoS₂–SPAN–CNT electrodes (Fig. 11a) [144]. First, PAN, CNT, and MeIM electrospun to obtain PAN–CNT–MeIM films. Adding into the salt solution containing Co at room temperature, ZIF-67@PAN–CNT film is obtained. After curing, the SPAN–CNT decorated with CoS₂ film, which had a high sulfur load of 4.6 mg cm⁻² (only 90 mm thick). As a result, the CoS₂–SPAN–CNT electrode led to a capacity of 1240 mA h g⁻¹ at 0.2 C. The modification of ZIF-67 in the structure helped to restrain the expansion of the fiber and the thickening of the membrane. Meanwhile, the introduction of CoS₂ accelerated the redox kinetics of sulfur. According to the SEM images of the PAN–CNT–Meim membrane shown in Fig. 11b, the average fiber diameter of the PAN–CNT–Meim was about 430 nm. After modification of ZIF-67, the average diameter of the ZIF-67@PAN–CNT membrane increased to 714 nm (Fig. 11c). The resulting vulcanized CoS₂ fixed on the surface of the SPAN–CNT film (Fig. 11d). Liu's research groups also reported and synthesized the MOFs modified gel F-doped poly-m-phenyleneisophthalamide (PMIA) nanofiber membranes. PMIA of ZIF-67 and Cu-BTC is combined by blending electrospinning, as shown in Fig. 11e [145]. The electrochemical performance and safety of Li–S cells improved by the modified fiber film. F-doping is mainly contributed to the formation of a gel state and reduced the average fiber diameter of the prepared membrane. These membrane materials had smaller pore sizes, higher porosity, and excellent ionic conductivity. MOF doping enhanced the chemical adsorption of lithium polysulfide and showed a good catalytic effect in the redox reaction. In terms of the adsorption of poly lithium sulfide, the F-doped and MOFs co-doped membrane was beneficial to physically capture poly lithium sulfide, reduced the lithium dendrites, and helped to achieve uniform lithium deposition on the surface of lithium electrode during the process of charging and discharging. Both F-ZIF-67 and F-Cu-BTC-doped modified films demonstrated excellent electrochemical performance, with discharge capacities up to 1267.5 and 1272.2 mAh g⁻¹ at 0.5 C. It is possible to functionalize MOFs and effectively improve the performance of lithium–sulfur batteries.

Sodium-Ion Batteries

Sodium-ion batteries (SIBs) have appealed much attention, because harmless properties, low cost, rich sodium resources, and electrochemical storage mechanism are similar to LIBs. However, sodium-ion have more radius than lithium-ion, which seriously affected the poor circulation and low kinetics of the electrode during the process of sodium/modification. The design and development of unique materials with cavity heterostructure could reduce the volume expansion and increase the electron transport path in the cycle process. MOFs are an ideal template for creating hollow structures. In this summary, MOFs have been used as a template to reasonably design the structure and apply it to the storage of sodium-ion batteries through electrospinning [146–150].

Ma et al. demonstrated hollow heterostructures (CoFe)Se₂ three-dimensional (3D) carbon frameworks (CNS) via electrospinning and selenization treatment. The preparation route is shown in Fig. 12a. ZIF-67 nanocube was a self-sacrificing template. ZIF-67 and [Fe(CN)₆]³⁻ are transformed into layered hollow ZIF-67/Co-Fe PBA in the cation-exchange method. A hollow ZIF-67/Co-Fe PBA grown on one-dimensional polyacrylonitrile (PAN) nanofiber framework and Co₃O₄/Fe₃O₄@CNS obtained by annealing in an Ar atmosphere. After the selenization process, it converted into nano chains (CoFe)Se₂@CNS composite materials [151]. The composite displayed remarkable cycling life and rate property in SIBs. After 3650 cycles and the current density of 5 A g⁻¹, the capacity retention rate was still 98.6%. Changing the current density from 0.1 to 8 A g⁻¹, the capacity decreased from 262.9 to 218.2 mA h g⁻¹. The reasons are as follows: (1) The ingeniously designed hollow heterostructure coupled with the carbon skeleton. The hollow internal heterostructure provided enough buffer space for the movement of sodium ions, efficiently liberated the mechanical stress attributing to the volume variation of the material itself, enhanced the transport of electrolyte ions, and shortens the distance of ion transmission. (2) The anisotropy of electron transport enhanced by the three-dimensional network to accelerate the reaction kinetics of sodium ions. (3) The interesting internal electric field at the heterojunction derived from the combination of N-type CoSe₂ and P-type FeSe₂, which created a built-in electric field at the heterojunction interface, accelerating Na⁺ migration and adding more active sites. (4) The coupling effect of heterogeneous structure formation reduced the pulverization of materials in the cycling process, thus forming a stable SEI film [152, 153]. Li et al. fabricated the hierarchical NiCo₂O₄/NiO/carbon nanofibers via an electrospinning and annealing strategy (Fig. 12b) [154]. Co salt and Ni salt mixed into PAN and PVP to get 1D polymer (Co/Ni) fibers, which immersed in 2-MeIM and obtained the polymer (Co/

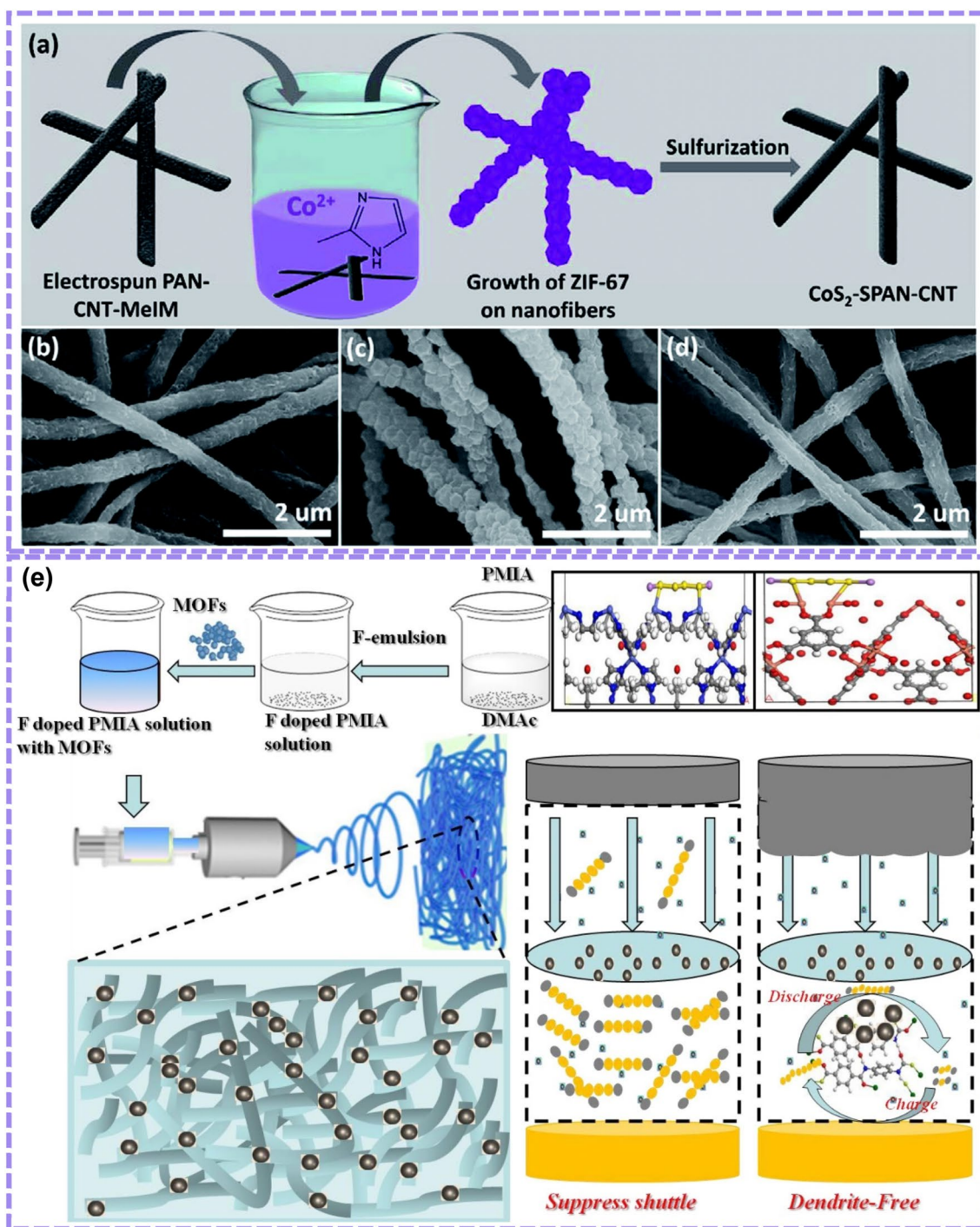


Fig. 11 Schematic diagram of the as-prepared composites and the morphology characterization in the lithium-sulfur battery. **a** Process flow diagram of CoS_2 -SPAN-CNT electrodes; SEM images of **b** PAN-CNT-MeIM, **c** ZIF-67@PAN-CNT; **d** CoS_2 -SPAN-CNT;

reprinted with permission from ref. [144], Copyright 2020, Royal Society of Chemistry; **e** the schematic illustration of the MOFs nanoparticles modified PMIA membrane; reprinted with permission from ref. [145], Copyright 2020, Elsevier

Ni)@Ni/Co-MOF. After the carbonization and oxidation, hierarchical $\text{NiCo}_2\text{O}_4/\text{NiO}/\text{carbon}$ nanofibers demonstrated a sodium-storage capacity of 210 mAh g^{-1} at 100 mA g^{-1} . The one-dimensional carbonized nanofibers composite

film inlaid with NiCo_2O_4 and NiO conductive particle and intertwined with each other to form a three-dimensional structure. It could effectively shorten the ion diffusion, and accelerated the diffusion kinetics along its one-dimensional

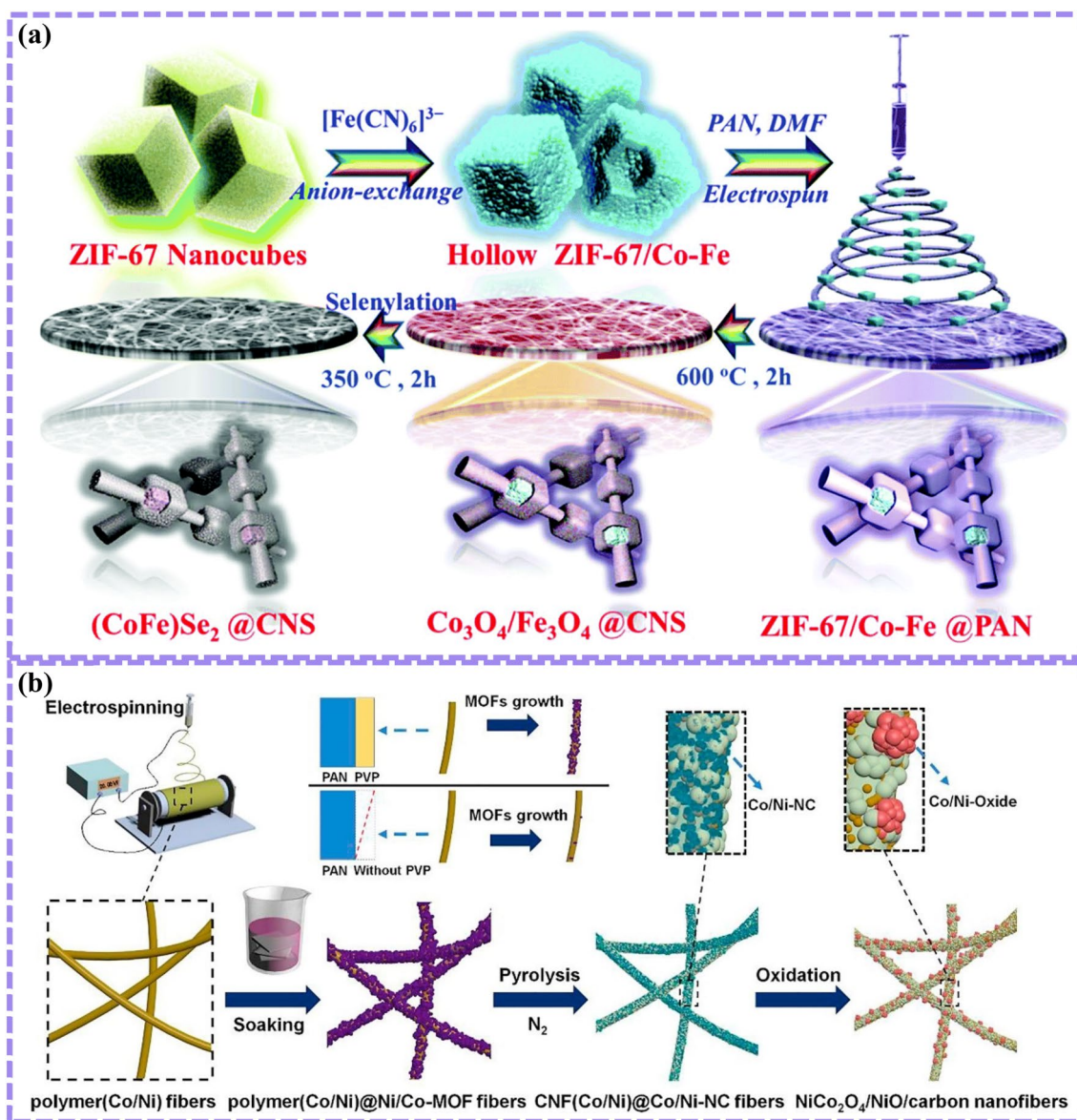


Fig. 12 Schematic illustration of the MOF-derived composite structure in sodium-ion batteries. **a** (CoFe)Se₂@CNS; reprinted with permission from ref. [151], Copyright 2020, Royal Society of Chemistry;

b NiCo₂O₄/NiO/carbon nanofibers; reprinted with permission from ref. [154], Copyright 2019, Elsevier

form of high-speed electron mobility. The evenly dispersed particles increased the electrolyte exposure surface, which improved the material utilization rate.

Jiang's group designed the hybrid of Fe₇S₈/N-doped carbon nanofibers (Fe₇S₈/N-CNFs) by electrospinning [155]. MIL-88A-Fe/PAN composite membrane obtained by directly adding MIL-88A-Fe to PAN for electrospinning (Fig. 13a). However, Fe₇S₈/N-CNFs demonstrated a high capacity of 649.9 mAh g⁻¹ at 0.2 A g⁻¹. The excellent electrochemical performance attributed to: the average diameter of Fe₇S₈ nanoparticles was 17 nm, which shorten the Na⁺ diffusion path; the one-dimensional carbon

network and three-dimensional carbon nanocage structure combined to enhance the conductivity of the composite; Fe₇S₈ was uniformly dispersed on the surface of the carbon fiber, which could effectively slow the agglomeration and volume expansion of Fe₇S₈ during the electrochemical reaction. It also provided more active sites for Na⁺ adsorption. Zhao et al. constructed a carbon-coated metal sulfur selenide solid-solution CoSSe nanosheet on carbon nanofiber (CNF@CoSSe@C) by electrospinning [156]. The electrospun polyacrylonitrile (PAN) nanofiber membrane was used as the precursor, and then, the ZIF-67 nanosheet was embedded in the PAN by immersion.

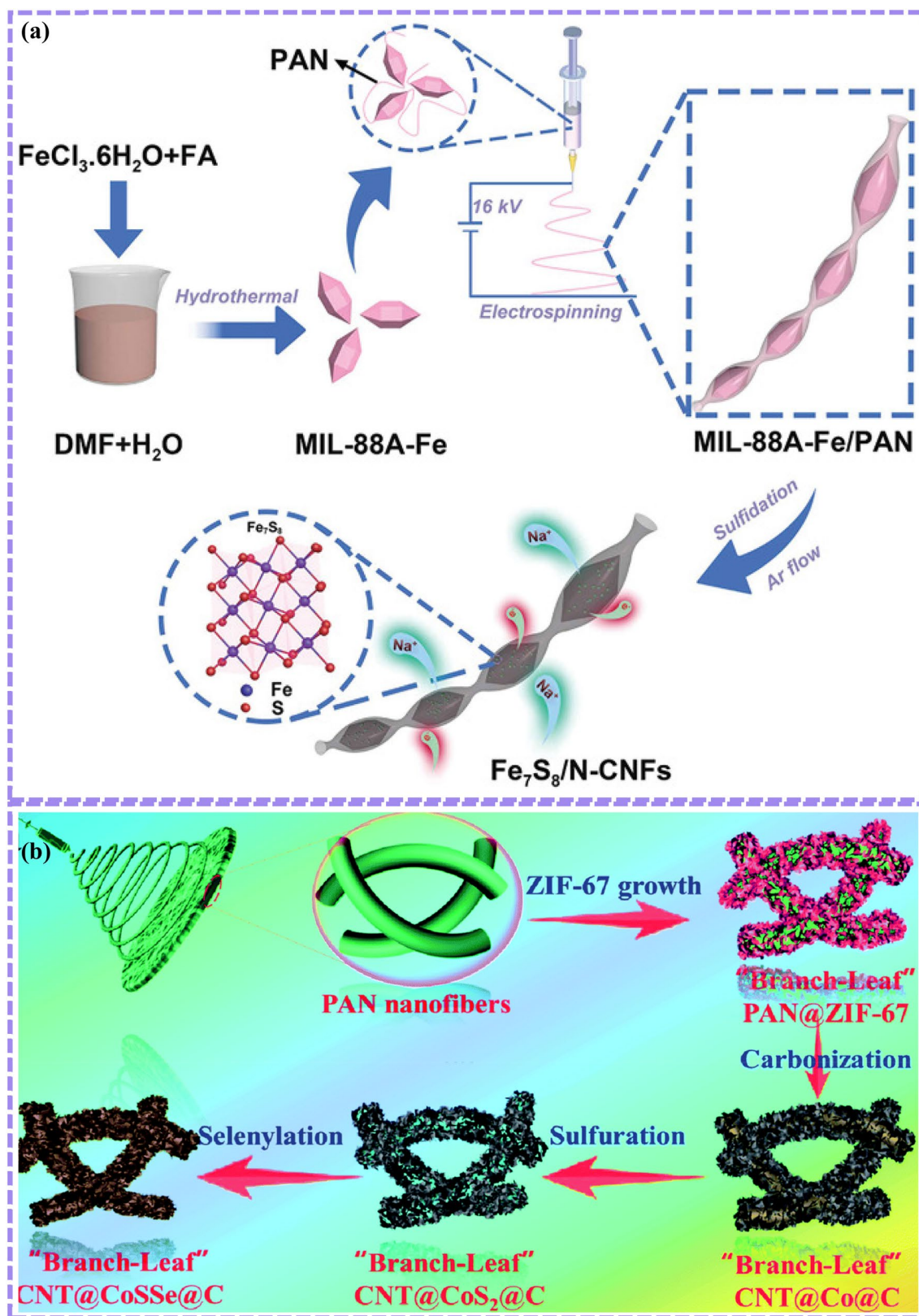


Fig. 13 Preparation process diagram of the as-prepared electrode in sodium-ion batteries. **a** $\text{Fe}_7\text{S}_8/\text{N-CNFs}$; reprinted with permission from ref. [155], Copyright 2021, Wiley-VC and **b** CNT@CoSSe@C ;

reprinted with permission from ref. [156], Copyright 2022, Royal Society of Chemistry

PAN@ZIF-67 was carbonized, vulcanized, and selenized to obtain a carbon-coated CoSSe nanosheet, grown on one-dimensional PAN (Fig. 13b). This structure formed a three-dimensional network structure of PAN as a branch and CoSSe@C as a leaf. CNF@CoSSe@C had a capacity of $479.4 \text{ mA h g}^{-1}$ at 1 A g^{-1} as the negative electrode of the SIBs. This carefully designed structure was conducive to enhancing the conductivity and mechanical strength of materials, forming more abundant electrochemical active sites, and the three-dimensional structure provided more channels for ion transport. DFT showed that this structure had the lowest migration barrier energy for sodium ions and accelerates the diffusion of Na^+ .

Potassium-Ion Batteries

Potassium-ion batteries (PIBs) have become a new type of energy storage device and attract much attention because of their low redox potential, abundant reserves, and low cost. The combination of MOF and electrospinning to prepare potassium-ion battery electrode materials can effectively shorten the ion diffusion path. MOFs as a template could provide a stable structural framework for its derivative materials to alleviate volume expansion and improves conductivity.

Zhang et al. fabricated $\text{Co}_{0.85}\text{Se@CNFs}$ nanoboxes by embedding Co-MOF into PAN for carbonization and selenization (Fig. 14a). The $\text{Co}_{0.85}\text{Se@CNFs}$ flexible films had

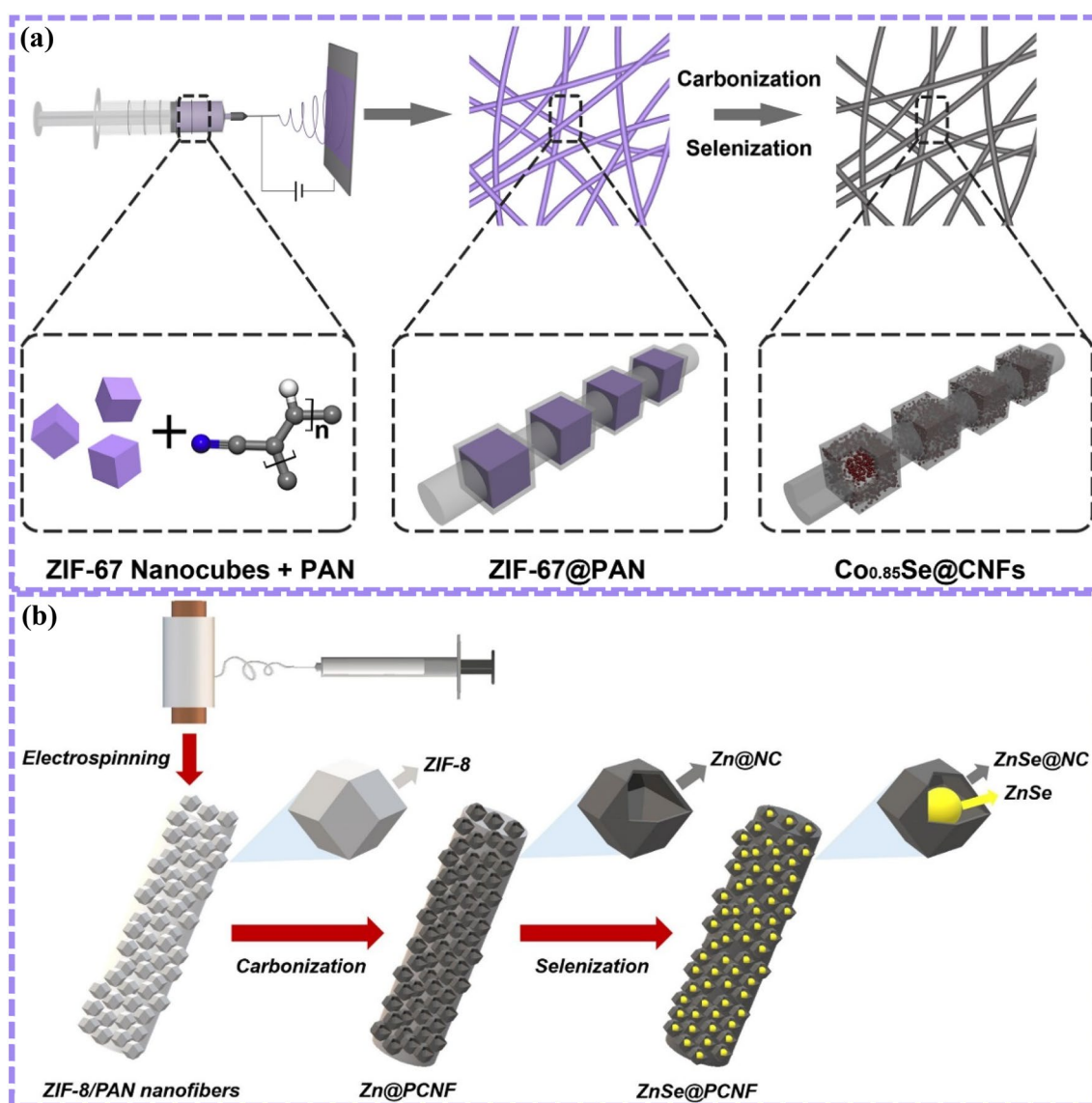


Fig. 14 The synthetic process of MOF-derived nanostructure in potassium-ion batteries. **a** $\text{Co}_{0.85}\text{Se@CNFs}$; reprinted with permission from ref. [157], Copyright 2020, Elsevier; **b** ZnSe@PCNF composite; reprinted with permission from ref. [158], Copyright 2021, Elsevier

a high active material load [157]. In addition, the composite nanobox structure had a large internal space, which was convenient for K^+ diffusion and transmission, and slowed down the deformation of $Co_{0.85}Se$ in the electrochemical reaction. Using carbon encapsulation, $Co_{0.85}Se$ restricted to a certain area to prevent material crushing. Thus, after 100 cycles, this nanocomposite film displayed a capacity of 353 mAh g^{-1} at 0.2 A g^{-1} , and with the current density increasing to 5 A g^{-1} a specific capacity of 166 mAh g^{-1} in PIBs. Park's group demonstrated the preparation process of $ZnSe@PCNF$ in Fig. 14b [158]. First, a diameter of 100 nm of ZIF-8/PAN as-obtained by the electrostatic spinning method and N-doped carbon film obtained by annealing treatment. After the selenization treatment, the $ZnSe@N$ -doped carbon ($ZnSe@NC$) material formed and displayed an excellent capacity of 270 mA h g^{-1} at 0.5 A g^{-1} . Using MOFs as precursors, a simple process uniformly confined

metal selenide nanoparticles to carbon fibers. In addition, metal Zn transformed into $ZnSe$ with excellent potassium-ion storage capacity through the selenization process. This structure provided enough active sites for K^+ to store energy and shorten the diffusion path of ions. N-doped carbon materials helped to restrain the volume expansion of $ZnSe$ nanocrystals in electrochemical reactions and increased their high conductivity.

Lu's group grew MoP ultrafine nanoparticles on N, P co-doped carbon nanofibers (MoP@NPCNFs) by electrospinning (Fig. 15a) [159]. N, P co-doped carbon nanofibers obtained through the carbonization of ZIF-8 and PAN electrospinning. After being immersed in ammonia molybdate and phosphorization process, MoP@NPCNFs carbon nanofibers are prepared. It displayed a noteworthy capacity of 320 mAh g^{-1} at 100 mA g^{-1} , and 220 mAh g^{-1} at 2 A g^{-1} . Thus, the strong interaction between MoP particles

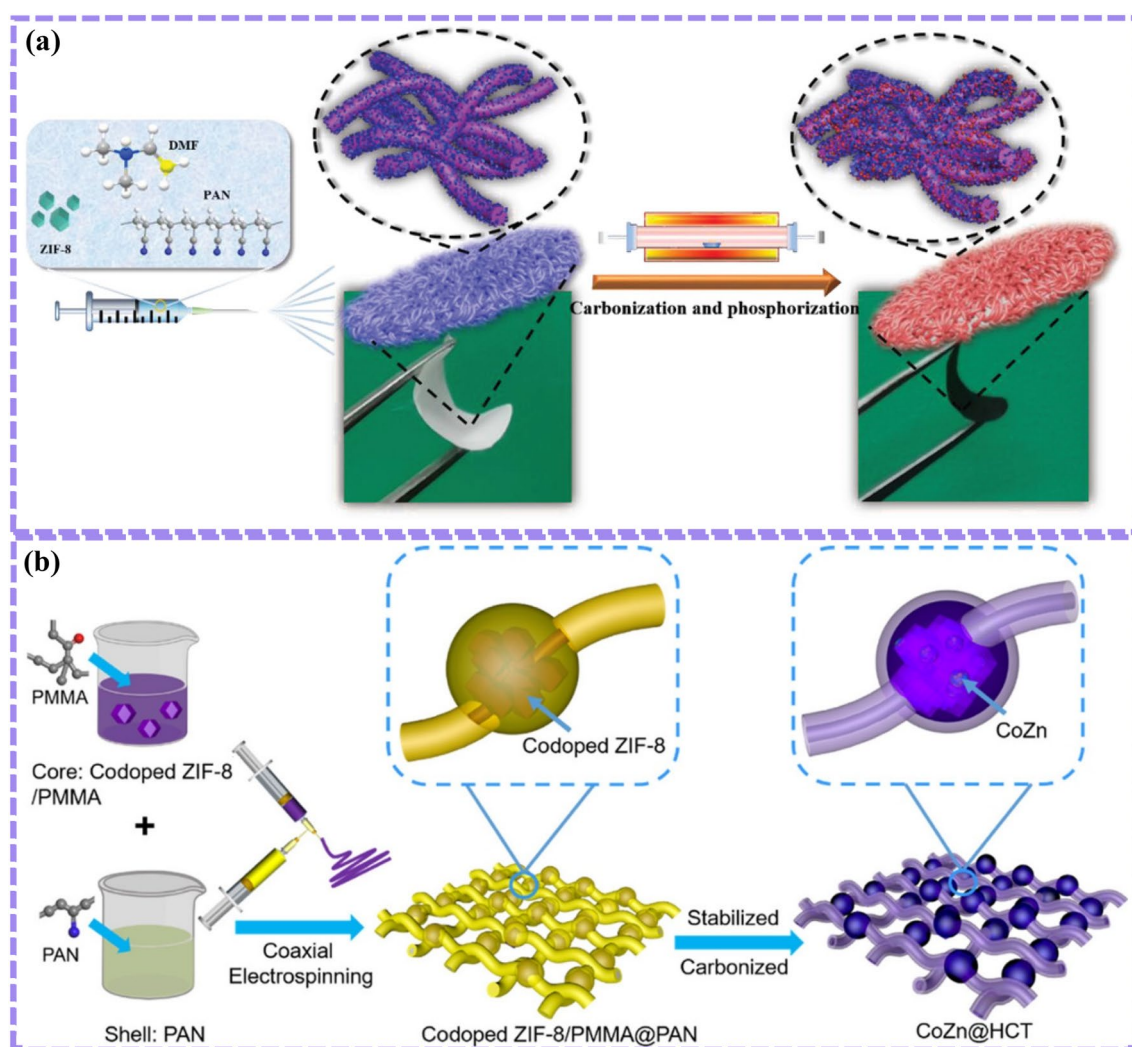


Fig. 15 Preparation process diagram of MOF-derived nanostructure in potassium-ion batteries. **a** MoP@NPCNFs; reprinted with permission from ref. [159], Copyright 2020, Wiley-VC; **b** CoZn@HCT composite; reprinted with permission from ref. [160], Copyright 2021, Elsevier

and NPCNFs effectively alleviated electrode fragmentation and agglomeration; the three-dimensional network structure increased the contact area between the material and the electrolyte, accelerated the reaction kinetics, and had excellent rate performance; Flexible membrane electrodes can be used in flexible energy storage devices. Wang's group prepared the CoZn nanoparticle structure and mosaicked it in hollow carbon tubes (CoZn@HCT) [160]. By the coaxial electrospinning, co-doped ZIF-8/polymethyl methacrylate (PMMA) and polyacrylonitrile (PAN) were the inner axes and the outer layer (Fig. 15b). After annealing, CoZn nanoparticles coated in N-doped hollow carbon tubes. A cavity existed in the CoZn@HCT structure to accommodate the volume change of K metal during the cycle. The adsorption energy of CoZn and K^+ was the lowest by DFT calculation, which improved the interaction between K and the electrode. The conductive CoZn@HCT skeleton can effectively reduce the local current density and adjust the uniform distribution of ions.

Conclusion and Future Perspectives

MOFs and electrospinning are combined to give full play to the superiorities of both to flexibly design composite nanomaterials with controllable pore size and structure. Noteworthy, these kind of composite nanofibers have plenty of advantages on open pore volume and well-proportioned distribution of metal active sites. The one-dimensional fiber and three-dimensional carbon skeleton facilitate ion storage and transportation, which contribute to boosting the conductivity of the as-obtained composite. The well-designed composite nanomaterials are diffusely applied to energy storage. Although the combination of MOFs and electrospinning in the field of energy storage has made some research progress, it has both advantages and challenges in the main preparation methods.

(1) The as-obtained MOF was first put into the electrospinning solution, and then, electrospinning was carried out to prepare the composite material. Noteworthy, the materials synthesized by this preparation route have the advantages of simple synthesis, excellent mechanical properties of composite films, and adjustable structures and functions. However, they also has certain limitations. (i) The presence of MOFs in composite films. MOFs have a significant effect on the conductivity of electrospinning precursors, and the addition of too many MOF crystals has a significant effect on conductivity. (ii) The size of the MOFs themselves needs to match the size of the electrospun fiber diameter, and the size of the MOFs is too large, which can easily lead to an uneven spinning effect.

(2) MOF were grown on the electrospun polymer film or carbon-based composite films by hydrothermal or other methods. Compared with the previous direct blending electrospinning method, MOFs were grown directly on the surface of the polymer membrane, and the pores of the MOFs were not covered by polymer fibers. However, the limitations lie in the following: (i) The solvent of the electrospun solution easily affects the nucleation and growth process of the MOF. The selected electrospinning solution must not react with or corrode MOFs, to ensure that the structure of MOFs is not destroyed. High temperature tends to make MOFs undergo a phase transition. (ii) Long reaction times and excessive temperatures may affect the stability of the polymer film.

(3) The MOF polymer composite film was annealed to obtain the derived-MOF composite fiber material. (i) After heat treatment, some metal ions of MOFs remain in the structure, resulting in an increase in the overall mass of the electrode material. (ii) Heteroatoms in organic ligands are easy to directly sublime due to high temperature, so doping is reduced. Therefore, in subsequent studies, it is necessary to further explore in detail the time and temperature of MOF structure carbonization to maximize the retention of heteroatoms. (iii) The mechanical properties of some composite films are partially reduced after heat treatment.

In addition to solving the above problems, there are several ways to broaden the application of MOFs and classical spinning composites.

(1) Development of new composite materials: More than 20,000 types of MOFs have been reported. Different MOFs have different pore structures and can accommodate electrolyte ions of different sizes in electrochemical reactions. The composite material is composed of different types of MOF fibers, which enriches the diversity of electrode materials. It is worth noting that some MOFs have the disadvantages of poor conductivity and low crystallinity [161, 162]. However, with the advent of DFT meters, MD simulations, machine learning, and the use of emerging computer techniques, the relationship between the structure of different MOFs and electrons can be predicted. These ways play a screening role in electrode materials. Through theoretical simulations, both orbital interactions of orbital overlap between metal ions and organic ligands and π - π superposition between efficient ligands and ligands enhance the conductivity of MOFs. Moreover, through the reasonable selection of organic ligands and metal ions, MOFs have as a small molecular weight and many redox active sites as possible, and finally obtain satisfactory capacity.

- (2) Increase of electrochemical capacity: Through material design, the electrochemical performance of MOF fiber membranes can be improved. (i) By changing the structure and shape of the nanofibers (special nanostructures, such as hollow structures, core–shell structures, brush-like structures), more energy storage active sites are added to facilitate the transport of electrons. (ii) Through interface engineering, defect construction, and electronic structure regulation, more interfaces are provided for electrochemical reactions.
- (3) Stability of electrode materials: The stability of MOFs in water, chemical solvents, and heat is still not satisfactory. As the pore size increases, the chemical and thermal stability usually deteriorate. During the electrochemical process of MOFs, whether there is fragmentation and phase transition is a question that needs to be considered in follow-up research. In situ characterization tests can be used to record whether the structure of the electrode material changes during the electrochemical reaction, proving the electrochemical reaction mechanism effectively. Similarly, precise control of the preparation of MOF derivative structure must be carried out. Therefore, the products produced after cyclic testing can be characterized in subsequent studies.
- (4) Optimizing the material configuration: MOFs, derived-MOFs materials, and electrospun carbon fiber structures have different energy storage mechanisms. At the initial stage of material design, the ratio of composite materials is optimized to maximize the electrochemical performance of composite materials. Moreover, usually electrospinning precursor solutions contain organic components, and composite materials containing organic components are directly used, and energy storage devices are polluted in the process of later recycling and processing. However, although no organic solution technically of melt electrospinning can avoid these problems, high system viscosity has an impact on nanofiber production.
- (5) Optimize production costs: Because of the high price of organic ligands, composite membrane materials have not been industrialized. Therefore, reducing the cost is also a big test of the application of composite membrane materials. Finally, industrializing electrospinning remains a challenge. At present, most electrospinning technologies use single-needle electrospinning. However, it focuses on the research and use of various multi-needle/multi-jet electrospinning methods, which is convenient for the rapid and large-scale preparation of complex fibers [163–165].

By solving the above problems, MOF composite fibers can achieve better performances in more fields. To sum up,

MOFs and their derived materials are used to reasonably design and construct functional heterogeneous fiber structures through electrostatic spinning, and they may have uses in the energy storage. Finally, it is hoped that MOF and its derived nanofibers will be applied industrially from the laboratory as soon as possible.

Supplementary Information The online version contains supplementary material available at <https://doi.org/10.1007/s42765-023-00287-3>.

Acknowledgements Yao thanks the National Nature Science Foundation of China (21871066) and China Scholarship Council (CSC, No. 202006120429). S.Y. acknowledges Ms. Xin Luo for her support and encouragement during my study and life.

Data availability The data used in this study will be made available upon request to the corresponding authors.

Declarations

Conflict of Interest The authors declare no conflict of interest.

References

1. Chu S, Cui Y, Liu N. The path towards sustainable energy. *Nat Mater.* **2017**;16:16–22.
2. Liu XG, Zhang Y, Guo XT, Pang H. Electrospun metal–organic framework nanofiber membranes for energy storage and environmental protection. *Adv Fiber Mater.* **2022**;4:1463–85.
3. Guo Y, Bae J, Fang Z, Li P, Zhao F, Yu G. Hydrogels and hydrogel-derived materials for energy and water sustainability. *Chem Rev.* **2020**;120:7642–707.
4. Fang C, Lu B, Pawar G, Zhang M, Cheng D, Chen S, et al. Pressure-tailored lithium deposition and dissolution in lithium metal batteries. *Nat Energy.* **2021**;6:987–94.
5. Jia H, Liu KY, Lam Y, Tawiah B, Xin JH, Nie WQ, et al. Fiber-based materials for aqueous zinc ion batteries. *Adv Fiber Mater.* **2023**;5:36–58.
6. Lyu Z, Lim GJH, Koh JJ, Li Y, Ma Y, Ding J, et al. Design and manufacture of 3D printed batteries. *Joule.* **2021**;5:89–114.
7. Zhu YF, Tang ZY. Conductive 2D MOF coupled with super protonic conduction and interfacial pseudo-capacitance. *Matter.* **2020**;2:798–800.
8. Shi FY, Chen CH, Xu ZL. Recent advances on electrospun nanofiber materials for post-lithium ion batteries. *Adv Fiber Mater.* **2021**;3:275–301.
9. Yan J, Li S, Lan B, Wu Y, Lee PS. Rational design of nanostructured electrode materials toward multifunctional supercapacitors. *Adv Funct Mater.* **2020**;302:1902564.
10. Yao SY, Xing L, Dong YD, Wu X. Hierarchical WO₃@MnWO₄ core–shell structure for asymmetric supercapacitor with ultrahigh cycling performance at low temperature. *J Colloid Interface Sci.* **2018**;531:216–24.
11. Xing WN, Ma F, Li ZJ, Wang A, Liu MX, Han JG, et al. Edge effect-modulated exciton dissociation and charge transfer in porous ultrathin tubular graphitic carbon nitride for boosting photoredox activity. *J Mater Chem A.* **2022**;10:18333.
12. Cao XJ, Wang TZ, Jiao LF. Transition-metal (Fe Co, and Ni)-based nanofiber electrocatalysts for water splitting. *Adv Fiber Mater.* **2021**;3:210–28.

13. Gagnon KL, Perry HP, Clearfield A. Conventional and unconventional metal–organic frameworks based on phosphonate ligands: MOFs and UMOFs. *Chem Rev.* **2012**;112:1034–54.
14. Deng H, Grunder S, Cordova KE, Valente C, Furukawa H, Hmadeh M, et al. Large-pore apertures in a series of metal–organic frameworks. *Science.* **2012**;336:1018–54.
15. Yao SY, Jiao Y, Sun SF, Wang LX, Li PY, Chen G. Vertically Co-oriented Mn-metal–organic framework grown on 2D cation-intercalated manganese oxide via a self-sacrificing template process for a high-performance asymmetric supercapacitor. *ACS Sustain Chem Eng.* **2020**;8:3191–9.
16. Yaghi OM, Li H. Hydrothermal synthesis of a metal–organic framework containing large rectangular channels. *J Am Chem Soc.* **1995**;117:10401–2.
17. Li B, Wen HM, Cui YJ, Zhou W, Qian GD, Chen BL. Emerging multifunctional metal–organic framework materials. *Adv Mater.* **2016**;28(40):8819–60.
18. Lawson S, Rownaghi AA, Rezaei F. Carbon hollow fiber-supported metal–organic framework composites for gas adsorption. *Energy Technol.* **2018**;6:694–701.
19. Lee J, Kwak JH, Choe W. Evolution of form in metal–organic frameworks. *Nat Commun.* **2017**;8:14070.
20. Huo J, Marcello M, Garai A, Bradshaw D. MOF-polymer composite microcapsules derived from pickering emulsions. *Adv Mater.* **2013**;25:2717–22.
21. Doherty CM, Buso D, Hill AJ, Furukawa S, Kitagawa S, Falcaro P. Using functional nano-and microparticles for the preparation of metal–organic framework composites with novel properties. *Acc Chem Res.* **2014**;47:396–405.
22. Bai Y, Dou Y, Xie LH, Rutledge W, Li JR, Zhou HC. Zr-based metal–organic frameworks: design, synthesis, structure, and applications. *Chem Soc Rev.* **2016**;45:2327–67.
23. Xu G, Nie P, Dou H, Ding B, Li L, Zhang X. Exploring metal organic frameworks for energy storage in batteries and supercapacitors. *Mater Today.* **2017**;20(4):191–209.
24. Cui Y, Li B, He H, Zhou W, Chen B, Qian G. Metal–organic frameworks as platforms for functional materials. *Acc Chem Res.* **2016**;49(3):483–93.
25. Zhou HCJ, Kitagawa S. Metal–organic frameworks (MOFs). *Chem Soc Rev.* **2014**;43:5415–8.
26. Rodenas T, Luz I, Prieto G, Seoane B, Miro H, Corma A, et al. Metal–organic framework nanosheets in polymer composite materials for gas separation. *Nat Mater.* **2015**;14:48–55.
27. Li X, Liu Y, Wang J, Gascon J, Li J, Bruggen BV. Metal–organic frameworks based membranes for liquid separation. *Chem Soc Rev.* **2017**;46:7124–44.
28. Lustig WP, Mukherjee S, Rudd ND, Desai AV, Li J, Ghosh SK. Metal–organic frameworks: functional luminescent and photonic materials for sensing applications. *Chem Soc Rev.* **2017**;46:3242–85.
29. Cao X, Tan C, Sindoro M, Zhang H. Hybrid micro-/nano-structures derived from metal–organic frameworks: preparation and applications in energy storage and conversion. *Chem Soc Rev.* **2017**;46:2660–77.
30. Kaneti YV, Tang J, Salunkhe RR, Jiang X, Yu A, Wu KC, Yamauchi Y. Nanoarchitected design of porous materials and nanocomposites from metal–organic frameworks. *Adv Mater.* **2017**;29:1604898.
31. Sun X, Suarez AIO, Meijerink M, Deelen TV, Ould-Chikh S, Zecevic J, et al. Manufacture of highly loaded silica-supported cobalt fischer-tropsch catalysts from a metal organic framework. *Nat Commun.* **2017**;8:1680.
32. Salunkhe RR, Kaneti YV, Kim J, Kim JH, Yamauchi Y. Nano-architectures for metal–organic framework-derived nanoporous carbons toward supercapacitor applications. *Acc Chem Res.* **2016**;49:2796–806.
33. Hu M, Reboul J, Furukawa S, Torad NL, Ji Q, Srinivasu P, et al. Direct carbonization of Al-based porous coordination polymer for synthesis of nanoporous carbon. *J Am Chem Soc.* **2012**;134:2864–7.
34. Tang J, Yamauchi Y. Carbon materials: MOF morphologies in control. *Nat Chem.* **2016**;8:638–9.
35. Pachfule P, Shinde D, Majumder M, Xu Q. Fabrication of carbon nanorods and graphene nanoribbons from a metal–organic framework. *Nat Chem.* **2016**;8:718–24.
36. Zhang Y, Su Q, Xu W, Cao G, Wang Y, Pan A, et al. A confined replacement synthesis of bismuth nanodots in MOF derived carbon arrays as binder-free anodes for sodium-ion batteries. *Adv Sci.* **2019**;6:1900162.
37. Liu P, Redekop E, Gao X, Liu WC, Olsbye U, Somorjai GA. Oligomerization of light olefins catalyzed by bronsted-acidic metal–organic framework-808. *J Am Chem Soc.* **2019**;141(29):11557–64.
38. Li J, Jiao C, Zhu J, Zhong L, Kang T, Aslam S, et al. Hybrid co-based MOF nanoboxes/CNFs interlayer as microreactors for polysulfides-trapping in lithium–sulfur batteries. *J Energy Chem.* **2021**;57:469–76.
39. Khodayari P, Jalilian N, Ebrahimzadeh H, Amini S. Tracelevel monitoring of anti-cancer drug residues in wastewater and biological samples by thin-film solid-phase micro-extraction using electrospun polyfam/Co-MOF-74 composite nanofibers prior to liquid chromatography analysis. *J Chromatogr A.* **2021**;1655:462484.
40. Peng J, Tao J, Liu Z, Yang Y, Yu L, Zhang M, et al. Ultra-stable and high capacity flexible lithium-ion batteries based on bimetallic MOFs derivatives aiming for wearable electronic devices. *Chem Eng J.* **2021**;417: 129200.
41. Niu Q, Guo J, Chen B, Nie J, Guo X, Ma G. Bimetal-organic frameworks/polymer core–shell nanofibers derived heteroatom-doped carbon materials as electrocatalysts for oxygen reduction reaction. *Carbon.* **2017**;114:250–60.
42. Piri-Moghadam H, Alam MN, Pawliszyn J. Review of geometries and coating materials in solid phase microextraction: opportunities, limitations, and future perspectives. *Anal Chim Acta.* **2017**;984:42–65.
43. Efome JE, Rana D, Matsuura T, Lan CQ. Insight studies on metal–organic framework nanofibrous membrane adsorption and activation for heavy metal ions removal from aqueous Solution. *ACS Appl Mater Interfaces.* **2018**;10:18619–29.
44. Topuz F, Abdulhamid MA, Hardian R, Holtzl T, Szekely G. Nanofibrous membranes comprising intrinsically microporous polyimides with embedded metal–organic frameworks for capturing volatile organic compounds. *J Hazard Mater.* **2022**;424: 127347.
45. Wendorff JH, Agarwal S, Greiner A. Electrospinning: materials, processing, and applications. Hoboken: John Wiley & Sons; 2012.
46. Tucker N, Stanger JJ, Staiger MP, Razzaq H, Hofman K. The history of the science and technology of electrospinning from 1600 to 1995. *J Eng Fiber Fabr.* **2012**;7:63–73.
47. Lin J, Wang X, Ding B, Yu J, Sun G, Wang M. Biomimicry via electrospinning. *Crit Rev Solid State.* **2012**;37:94–114.
48. Greiner A, Wendorff JH. Electrospinning: a fascinating method for the preparation of ultrathin fibers. *Angew Chem Int Ed.* **2007**;46(30):5670–703.
49. Zeleny J. The electrical discharge from liquid points, and a hydrostatic method of measuring the electric intensity at their surfaces. *Phys Rev.* **1914**;11(2):69–91.
50. Zeleny J. Instability of electrified liquid surfaces. *Phys Rev.* **1917**;10(1):1–6.
51. Nasir AM, Awang N, Jaafar J, Is AF, Othman MHD, Rahman MA, et al. Recent progress on fabrication and application of

- electrospun nanofibrous photocatalytic membranes for wastewater treatment: a review. *J Water Process Eng.* **2021**;40:101878.
52. Zeleny J. The electrical discharge from liquid points, and a hydrostatic method of measuring the electric intensity at their surface. *Phys Rev.* **1914**;3:69–91.
 53. Xue JJ, Wu T, Dai YQ, Xia YN. Electrospinning and electrospun nanofibers: methods, materials, and applications. *Chem Rev.* **2019**;119:5298–415.
 54. Dou Y, Zhang W, Kaiser A. Electrospinning of metal–organic frameworks for energy and environmental applications. *Adv Sci.* **2020**;7(3):1902590.
 55. Liu H, Cao C, Huang J, Chen Z, Chen G, Lai Y. Progress on particulate matter filtration technology: basic concepts, advanced materials, and performances. *Nanoscale.* **2020**;12:437–53.
 56. Boriboon D, Vongsetskul T, Limthongkul P, Kobsiriphat W, Tammawat P. Cellulose ultrafine fibers embedded with titania particles as a high performance and eco-friendly separator for lithium-ion batteries. *Carbohydr Polym.* **2018**;189:145–51.
 57. Miao TE, Zhu GN, Hou H, Xia YY, Liu T. Electrospun polyimide nanofiber-based nonwoven separators for lithium-ion batteries. *J Power Sour.* **2013**;226:82–6.
 58. Fu K, Gong Y, Dai J, Gong A, Han X, Yao Y, et al. Flexible, solid-state, ion-conducting membrane with 3D garnet nanofiber networks for lithium batteries. *Proc Natl Acad Sci.* **2016**;113:7094–9.
 59. Drozin VG. The electrical dispersion of liquids as aerosols. *J Colloid Sci.* **1955**;10:158–64.
 60. Vonnegut B, Neubauer RL. Production of monodisperse liquid particles by electrical atomization. *J Colloid Sci.* **1952**;7:616–22.
 61. Wang X, Ding B, Sun G, Wang M, Yu J. Electro-spinning/netting: a strategy for the fabrication of three-dimensional polymer nano-fiber/nets. *Prog Mater Sci.* **2013**;58:1173–243.
 62. Woodruff MA, Hutmacher DW. The return of a forgotten polymer polycaprolactone in the 21st century. *Prog Polym Sci.* **2010**;35:1217–56.
 63. Pan ZJ, Liu HB, Wan QH. Morphology and mechanical property of electrospun PA 6/66 copolymer filament constructed of nanofibers. *J Fiber Bioeng Inf.* **2008**;1:47–54.
 64. Sun Z, Zussman E, Yarin AL, Wendorff JH, Greiner A. Compound core–shell polymer nanofibers by co-electrospinning. *Adv Mater.* **2003**;15:1929–32.
 65. Zhang L, Fang M. Nanomaterials in pollution trace detection and environmental improvement. *Nano Today.* **2010**;5:128–42.
 66. Mou F, Guan JG, Shi W, Sun Z, Wang S. Oriented contraction: a facile nonequilibrium heat treatment approach for fabrication of maghemite fiber-in-tube and tube-in-tube nanostructures. *Langmuir.* **2010**;26:15580–5.
 67. Hiroshi K, Bin D, Takayuki N, Hiroki T, Seimei S. Multi-core cable-like TiO₂ nanofibrous membranes for dye-sensitized solar cells. *Nanotechnology.* **2007**;18:165604.
 68. Yang SY, Zhu PN, Nair AS, Ramakrishna S. Rice grain-shaped TiO₂ mesostructures-synthesis, characterization and applications in dye-sensitized solar cells and photocatalysis. *J Mater Chem.* **2011**;21:6541–8.
 69. Kessick R, Tepper G. Microscale polymeric helical structures produced by electrospinning. *Appl Phys Lett.* **2004**;84:4807–9.
 70. Shin MK, Kim SI, Kim SJ. Controlled assembly of polymer nanofibers: from helical springs to fully extended. *Appl Phys Lett.* **2006**;88:223109.
 71. Koombhongse S, Liu W, Reneker DH. Flat polymer ribbons and other shapes by electrospinning. *J Polym Sci Pol Phys.* **2001**;39:2598–606.
 72. Jin Y, Yang D, Kang D, Jiang X. Fabrication of necklace-like structures via electrospinning. *Langmuir.* **2010**;26:1186–90.
 73. Lu X, Zhang D, Zhao Q, Wang C, Zhang W, Wei Y. Large-scale synthesis of necklace-like single crystalline PbTiO₃ nanowires. *Macromol Rapid Comm.* **2006**;27:76–80.
 74. Zhao Y, Cao X, Jiang L. Bio-mimic multichannel microtubes by a facile method. *J Am Chem Soc.* **2007**;129:764–5.
 75. Chen H, Wang N, Di J, Zhao Y, Song Y, Jiang L. Nanowire-in-microtube structured core/shell fibers via multifluidic coaxial electrospinning. *Langmuir.* **2010**;26:11291–6.
 76. Chang ZJ. “Firecracker-shaped” ZnO/polyimide hybrid nanofibers via electrospinning and hydrothermal process. *Chem Commun.* **2011**;47:4427–9.
 77. Li D, Xia Y. Direct fabrication of composite and ceramic hollow nanofibers by electrospinning. *Nano Lett.* **2004**;4:933–8.
 78. Wu J, Wang N, Zhao Y, Jiang L. Electrospinning of multilevel structured functional micro-/nanofibers and their applications. *J Mater Chem.* **2013**;1:7290–305.
 79. Huang ZM, Zhang YZ, Kotaki M, Ramakrishna S. A review on polymer nanofibers by electrospinning and their applications in nanocomposites. *Compos Sci Technol.* **2003**;63:2223–53.
 80. Zhu X, Cui W, Li X, Jin Y. Electrospun fibrous mats with high porosity as potential scaffolds for skin tissue engineering. *Biomacromol.* **2008**;9:1795–801.
 81. Chevalier S, Lavielle N, Hatton BD, Bazylak A. Novel electrospun gas diffusion layers for polymer electrolyte membrane fuel cells: Part I. Fabrication, morphological characterization, and in situ performance. *J Power Sour.* **2017**;352:272–80.
 82. Mohamed IMA, Dao VD, Yasin AS, Barakat NAM, Choi HS. Design of an efficient photoanode for dye-sensitized solar cells using electrospun one-dimensional GO/N-doped nanocomposite SnO₂/TiO₂. *Appl Surf Sci.* **2017**;400:355–64.
 83. Aravindan V, Sundaramurthy J, Kumar SP, Lee YS, Ramakrishna S, Madhavi S. Electrospun nanofibers: a prospective electro-active material for constructing high performance Li-ion batteries. *Chem Commun.* **2015**;51:2225–34.
 84. Singh N, Salam Z, Sivasankar N, Subramania A. ZnSe quantum dots sensitized electrospun ZnO nanofibers as an efficient photoanode for improved performance of QDSSC. *Mat Sci Semicon Proc.* **2017**;64:16–23.
 85. Kharel K, Gangineni R, Ware L, Lu Y, Wujcik EK, Wei S, et al. Dehydrogenation properties of ammonia borane-polyacrylamide nanofiber hydrogen storage composites. *J Mater Sci.* **2017**;52:4894–902.
 86. Xu T, Du HS, Liu HY, Liu W, Zhang XY, Si CL, Liu PW, Zhang K. Advanced nanocellulose-based composites for flexible functional energy storage devices. *Adv Mater.* **2021**;33:2101368.
 87. Iqbal N, Wang X, Babar AA, Yan J, Yu J, Park SJ, Ding B. Polyaniline enriched flexible carbon nanofibers with core–shell structure for high-performance wearable supercapacitors. *Adv Mater Interfaces.* **2017**;4:1700855.
 88. Furukawa S, Reboul J, Diring S, Sumida K, Kitagawa S. Structuring of metal–organic frameworks at the mesoscopic/macroscale. *Chem Soc Rev.* **2014**;43:5700–34.
 89. Liu G, Liu C, Zhang W, Qiu S, Yi V, Chernikova Z, et al. Enhanced CO₂/CH₄ separation performance of a mixed matrix membrane based on tailored MOF-polymer formulations. *Adv Sci.* **2018**;5:800982.
 90. Stassen I, Burtch N, Talin A, Falcaro P, Allendorf M, Ameloot R. An updated roadmap for the integration of metal–organic frameworks with electronic devices and chemical sensors. *Chem Soc Rev.* **2017**;46:3185–241.
 91. Zhu QL, Xu Q. Metal–organic framework composites. *Chem Soc Rev.* **2014**;43:5468–512.
 92. Erucar I, Yilmaz G, Keskin S. Recent advances in metal–organic framework-based mixed matrix membranes. *Chem Asian J.* **2013**;8:1692–704.

93. Hossain MI, Udoh A, Grabick BE, Walton KS, Ritchie MC, Glover TG. Membrane-coated UiO-66 MOF adsorbents. *Ind Eng Chem Res.* **2019**;58:1352–62.
94. Lu AX, McEntee M, Browe MA, Hall MG, DeCoste JB, Peterson GW. MOF abric: electrospun nanofiber mats from PVDF/UiO-66-NH₂ for chemical protection and decontamination. *ACS Appl Mater Interfaces.* **2017**;9:13632–6.
95. McCarthy DL, Liu J, Dwyer DB, Troiano LJ, Boyer SM, DeCoste JB, et al. Electrospun metal–organic framework polymer composites for the catalytic degradation of methyl paraxon. *New J Chem.* **2017**;41:8748–53.
96. Liang H, Yao A, Jiao X, Li C, Chen D. Fast and sustained degradation of chemical warfare agent simulants using flexible self-supported metal–organic framework filters. *ACS Appl Mater Interfaces.* **2018**;10:20396–403.
97. Zhao J, Gong B, Nunn WT, Lemaire PC, Stevens EC, Sidi FI, et al. Conformal and highly adsorptive metal–organic framework thin films via layer-by-layer growth on ALD-coated fiber mats. *J Mater Chem A.* **2015**;3:1458–64.
98. Qu H, Wei S, Guo Z. Coaxial electrospun nanostructures and their applications. *J Mater Chem A.* **2013**;1:111513–28.
99. Nguyen TTT, Ghosh C, Hwang SG, Chanunpanich N, Park JS. Porous core/sheath composite nanofibers fabricated by coaxial electrospinning as a potential mat for drug release system. *Int J Pharm.* **2012**;439:296–306.
100. Wang S, Liu Q, Zhang Y, Wang S, Li Y, Yang Q. Preparation of a multifunctional material with super hydrophobicity, super paramagnetism, mechanical stability and acids-bases resistance by electrospinning. *Appl Surf Sci.* **2013**;279:150–8.
101. Zhang C, Shen L, Shen JQ, Liu F, Chen G, Tao R, et al. Anion-sorbent composite separators for high-rate lithium-ion batteries. *Adv Mater.* **2019**;31:1808338.
102. An S, Lee JS, Joshi BN, Jo HS, Titov K, Chang JS, et al. Freestanding fiber mats of zeolitic imidazolate framework 7 via one-step. Scalable electrospinning. *J Appl Polym Sci.* **2016**;133:43788.
103. Zhang YY, Yuan S, Feng X, Li HW, Zhou JW, Wang B. Preparation of nanofibrous metal–organic framework filters for efficient air pollution control. *J Am Chem Soc.* **2016**;138:5785–8.
104. Bai ZX, Liu SC, Chen P, Cheng GJ, Wu GY, Liu Y. Enhanced proton conduction of imidazole localized in one-dimensional Ni-metal–organic framework nanofibers. *Nanotechnology.* **2020**;31:125702.
105. Yao SY, Jiao Y, Lv CD, Kong Y, Ramakrishna S, Chen G. Lattice-strain engineering of CoOOH induced by NiMn-MOF for high-efficiency supercapacitor and water oxidation electrocatalysis. *J Colloid Interf Sci.* **2022**;623:1111–21.
106. Yang C, Yao Y, Lian YB, Chen YJ, Shah R, Zhao XH, et al. A double-buffering strategy to boost the lithium storage of botryoid MnOx/C anodes. *Small.* **2019**;15:1900015.
107. Yao SY, Zheng X, Zhang X, Xiao HH, Qu FY, Wu X. Facile synthesis of flexible WO₃ nanofibers as supercapacitor electrodes. *Mater Lett.* **2017**;186:94–7.
108. Li PY, Jiao Y, Yao SY, Wang LX, Chen G. Dual role of nickel foam in NiCoAl-LDH ensuring high-performance for asymmetric supercapacitors. *New J Chem.* **2019**;43:3139–45.
109. Wang LX, Jiao Y, Yao SY, Li PY, Wang R, Chen G. MOF-derived NiO/Ni architecture encapsulated into N-doped carbon nanotubes for advanced asymmetric supercapacitors. *Inorg Chem Front.* **2019**;6:1553–60.
110. Hou HS, Qiu XQ, Wei WF, Zhang Y, Ji XB. Carbon anode materials for advanced sodium-ion batteries. *Adv Energy Mater.* **2017**;7:1602898.
111. Ambrosi A, Chua CK, Latiff NM, Loo AH, Wong CHA, Eng AYS, et al. Graphene and its electrochemistry-an update. *Chem Soc Rev.* **2016**;45:2458–93.
112. Yang ZB, Ren J, Zhang ZY, Chen XL, Guan GZ, Qiu LB, et al. Recent advancement of nanostructured carbon for energy applications. *Chem Rev.* **2015**;115:5159–223.
113. Liu LL, Niu ZQ, Chen J. Unconventional supercapacitors from nanocarbon-based electrode materials to device configurations. *Chem Soc Rev.* **2016**;45:4340–63.
114. Zhao SH, Wu HH, Li YL, Li Q, Zhou JJ, Yu XB, et al. Core-shell assembly of carbon nanofibers and a 2D conductive metal–organic framework as a flexible free-standing membrane for high-performance supercapacitors. *Inorg Chem Front.* **2019**;6:1824–30.
115. Yao SY, Zhang X, Qu FY, Umar A, Wu X. Hierarchical WO₃ nanostructures assembled by nanosheets and their applications in wastewater purification. *J Alloys Compd.* **2016**;689:570–4.
116. Mukhiya T, Muthurasu A, Tiwari AP, Chhetri K, Chae SH, Kim H, et al. Integrating the essence of a metal–organic framework with electrospinning: a new approach for making a metal nanoparticle confined N-doped carbon nanotubes/porous carbon nanofibrous membrane for energy storage and conversion. *ACS Appl Mater Interfaces.* **2021**;13:23732–42.
117. Gong YJ, Chen RY, Xu H, Yu CY, Zhao X, Sun Y, et al. Polarity-assisted formation of hollow-frame sheathed nitrogen-doped nanofibrous carbon for supercapacitors. *Nanoscale.* **2019**;11:2492–500.
118. Azadmanjiri J, Srivastava VK, Kumar P, Nikzad M, Wang J, Yu A. Two-and three-dimensional graphene-based hybrid composites for advanced energy storage and conversion devices. *J Mater Chem A.* **2018**;6:702–34.
119. Xiao HH, Yao SY, Qu FY, Zhang X, Wu X. Electrochemical energy storage performance of heterostructured SnO₂@MnO₂ nanoflakes. *Ceram Int.* **2017**;43:1688–94.
120. Chen YM, Yu L, Lou XW. Hierarchical tubular structures composed of Co₃O₄ hollow nanoparticles and carbon nanotubes for lithium storage. *Angew Chem Int Ed.* **2016**;55:5990–3.
121. Han ZC, Zheng X, Yao SY, Xiao HH, Qu FY, Wu X. Donut-shaped Co₃O₄ nanoflakes grown on nickel foam with enhanced supercapacitive performances. *Appl Surf Sci.* **2016**;365:240–4.
122. Tian D, Song N, Zhong MX, Lu XF, Wang C. Bimetallic MOF nanosheets decorated on electrospun nanofibers for high-performance asymmetric supercapacitors. *ACS Appl Mater Interfaces.* **2020**;12:1280–91.
123. Samuel E, Joshi B, Kim MW, Kim Y, Swihart MT, Yoon SS. Hierarchical zeolitic imidazolate framework-derived manganese-doped zinc oxide decorated carbon nanofiber electrodes for high performance flexible supercapacitors. *Chem Eng J.* **2019**;371:657–65.
124. Feng J, Zhou H, Wang J, Bian T, Shao J, Yuan A. MoS₂ supported on MOF derived carbon with core–shell structure as efficient electrocatalysts for hydrogen evolution reaction. *Int J Hydrogen Energy.* **2018**;43:20538–45.
125. Shao J, Zhou H, Zhu M, Feng J, Yuan A. Facile synthesis of metal–organic framework-derived Co₃O₄ with different morphologies coated graphene foam as integrated anodes for lithium-ion batteries. *J Alloy Compd.* **2018**;768:1049–57.
126. Lee DK, Choi KS. Enhancing long-term photostability of BiVO₄ photoanodes for solar water splitting by tuning electrolyte composition. *Nat Energy.* **2017**;3:53–60.
127. Campagnol N, Romero-Vara R, Deleu W, Stappers L, Binne-mans K, Vos DED, et al. A hybrid supercapacitor based on porous carbon and the metal–organic framework MIL-100(Fe). *ChemElectroChem.* **2014**;1:1182–8.
128. Ji D, Zhou H, Tong Y, Wang J, Zhu M, Chen T, et al. Facile fabrication of MOF-derived octahedral CuO wrapped 3D graphene network as binder-free anode for high performance lithium-ion batteries. *Chem Eng J.* **2017**;313:1623–32.

129. Lu Y, Liu YB, Mo JM, Deng BL, Wang JX, Zhu YQ, et al. Construction of hierarchical structure of Co_3O_4 electrode based on electrospinning technique for supercapacitor. *J Alloys Compd.* **2021**;853: 157271.
130. Mukhiya T, Tiwari AP, Chhetri K, Kim T, Dahal B, Muthurasu A, et al. A metal–organic framework derived cobalt oxide/nitrogen-doped carbon nanotube nanotentacles on electrospun carbon nanofiber for electrochemical energy storage. *Chem Eng J.* **2021**;420: 129679.
131. Kim T, Subedi S, Dahal B, Chhetri K, Mukhiya T, Muthurasu A, et al. Homogeneous elongation of N-doped CNTs over nanofibrillated hollow-carbon-nanofiber: mass and charge balance in asymmetric supercapacitors is no longer problematic. *Adv Sci.* **2022**;9:2200650.
132. Lu X, Wang C, Favier F, Pinna N. Electrospun nanomaterials for supercapacitor electrodes: designed architectures and electrochemical performance. *Adv Energy Mater.* **2017**;7:1601301.
133. Sun H, Mei L, Liang J, Zhao Z, Lee C, Fei H, et al. Three-dimensional holey-graphene/niobia composite architectures for ultrahigh-rate energy storage. *Science.* **2017**;356:599–604.
134. Sun H, Xie S, Li Y, Jiang Y, Sun X, Wang B, et al. Large-area supercapacitor textiles with novel hierarchical conducting structures. *Adv Mater.* **2016**;28:8431.
135. Chen YM, Yu XY, Li Z, Paik U, Lou XW. Hierarchical MoS_2 tubular structures internally wired by carbon nanotubes as a highly stable anode material for lithium-ion batteries. *Sci Adv.* **2016**;2:1600021.
136. Chen G, Yan L, Luo H, Guo S. Nanoscale engineering of heterostructured anode materials for boosting lithium-ion storage. *Adv Mater.* **2016**;28:7580.
137. Zhang CL, Jiang ZH, Lu BR, Liu JT, Cao FH, Li H, et al. MoS_2 nanoplates assembled on electrospun polyacrylonitrile-metal organic framework-derived carbon fibers for lithium storage. *Nano Energy.* **2019**;61:104–10.
138. Du M, Rui K, Chang YQ, Zhang Y, Ma ZY, Sun WP, et al. Carbon necklace incorporated electroactive reservoir constructing flexible papers for advanced lithium-ion batteries. *Small.* **2018**;14:1702770.
139. Li Z, Tang BJ. Mn_3O_4 /nitrogen-doped porous carbon fiber hybrids involving multiple covalent interactions and open voids as flexible anodes for lithium-ion batteries. *Green Chem.* **2017**;19:5862–73.
140. Bian Y, Wang SJ, Jin DD, Wang RT, Chen C, Zhang L. A general anion exchange strategy to transform metal–organic framework embedded nanofibers into high-performance lithium-ion capacitors. *Nano Energy.* **2020**;75: 104935.
141. Dou YB, Zhang WJ, Kaiser A. Electrospinning of metal–organic frameworks for energy and environmental applications. *Adv Sci.* **2020**;7:1902590.
142. Cheong JY, Koo WT, Kim C, Jung JW, Kim ID. Feasible defect engineering by employing metal organic framework templates into one-dimensional metal oxides for battery applications. *ACS Appl Mater Interfaces.* **2018**;10(24):20540–9.
143. Xue SK, Yao SS, Jing MX, Zhu L, Shen XQ, Li TB, et al. Three-dimension ivy-structured MoS_2 nanoflakes-embedded nitrogen doped carbon nanofibers composite membrane as free-standing electrodes for Li/polysulfides batteries. *Electrochim Acta.* **2019**;299:549–59.
144. Razaq AA, Yuan XT, Chen YJ, Hu JP, Mu QQ, et al. Anchoring MOF-derived CoS_2 on sulfurized polyacrylonitrile nanofibers for high areal capacity lithium–sulfur batteries. *J Mater Chem A.* **2020**;8:1298.
145. Deng NP, Wang LY, Feng Y, Liu M, Li QX, Wang G, et al. Co-based and Cu-based MOFs modified separators to strengthen the kinetics of redox reaction and inhibit lithium-dendrite for long-life lithium–sulfur batteries. *Chem Eng J.* **2020**;388: 124241.
146. Lu JM, Zhao SY, Fan SX, Lv Q, Li J, Lv RT. Hierarchical SnS/SnS_2 heterostructures grown on carbon cloth as binder-free anode for superior sodium-ion storage. *Carbon.* **2019**;148:525–31.
147. Xie F, Zhang L, Su D, Jaroniec M, Qiao SZ. $\text{Na}_2\text{Ti}_3\text{O}_7$ @N-doped carbon hollow spheres for sodium-ion batteries with excellent rate performance. *Adv Mater.* **2017**;29:1700989.
148. Liu ZM, Lu TC, Song T, Yu XY, Lou XW, Paik U. Structure-designed synthesis of FeS_2 @C yolk-shell nanoboxes as a high-performance anode for sodium-ion batteries. *Energy Environ Sci.* **2017**;10:1576–80.
149. Bendi R, Kumar V, Bhavanasi V, Parida K, Lee PS. Metal organic framework-derived metal phosphates as electrode materials for supercapacitors. *Adv Energy Mater.* **2016**;6:1501833.
150. Dong SH, Li CX, Ge XL, Li ZQ, Miao XG, Yin LW. $\text{ZnS}-\text{Sb}_2\text{S}_3$ @C core-double shell polyhedron structure derived from metal–organic framework as anodes for high performance sodium ion batteries. *ACS Nano.* **2017**;11:6474–82.
151. Ma XQ, Chen J, Zhao WX. Construction of series-wound architectures composed of metal–organic framework-derived hetero-(CoFe)Se₂ hollow nanocubes confined into a flexible carbon skeleton as a durable sodium storage anode. *Nanoscale.* **2020**;12:22161–72.
152. Meng T, Gao JC, Liu YN, Zhu JH, Zhang H, Ma L, et al. Highly puffed Co_9S_8 /carbon nanofibers: a functionalized S carrier for superior Li-S batteries. *ACS Appl Mater Interfaces.* **2019**;30:8–26806.
153. Cao L, Gao XW, Zhang B, Ou X, Zhang JF, Luo WB. Bimetallic sulfide Sb_2S_3 @ FeS_2 hollow nanorods as high-performance anode materials for sodium-ion batteries. *ACS Nano.* **2020**;14:3610–20.
154. Zhang WM, Cao P, Zhang ZH, Zhao YJ, Zhang Y, Li L, et al. Nickel/cobalt metal–organic framework derived 1D hierarchical NiCo_2O_4 /NiO/carbon nanofibers for advanced sodium storage. *Chem Eng J.* **2019**;364:123–31.
155. Wang Y, Wen Z, Wang CC, Yang CC, Jian Q. MOF-derived Fe_7S_8 nanoparticles/N-doped carbon nanofibers as an ultra-stable anode for sodium-ion batteries. *Small.* **2021**;17:2102349.
156. Zhao WX, Gao LX, Ma XQ, Yue LC, Zhao DL, Li ZR, et al. An exquisite branch-leaf shaped metal sulfoselenide composite endowing an ultrastable sodium-storage lifespan over 10,000 cycles. *J Mater Chem A.* **2022**;10:16962.
157. Etogo CA, Huang HW, Hong H, Liu GX, Zhang L. Metal–organic-frameworks-engaged formation of $\text{Co}_{0.85}\text{Se}$ @C nanoboxes embedded in carbon nanofibers film for enhanced potassium-ion storage. *Energy Storage Mater.* **2020**;24:167–76.
158. Na JH, Kang YC, Park SK. Electrospun MOF-based ZnSe nanocrystals confined in N-doped mesoporous carbon fibers as anode materials for potassium ion batteries with long-term cycling stability. *Chem Eng J.* **2021**;425: 131651.
159. Yi ZB, Liu Y, Li YZ, Zhou LJ, Wang ZY, Zhang JQ, et al. Flexible membrane consisting of MoP ultrafine nanoparticles highly distributed inside N and P Co-doped carbon nanofibers as high-performance anode for potassium-ion batteries. *Small.* **2020**;16:1905301.
160. Cheng GZ, Liu S, Wang XJ, Li XR, Su YX, Shi J, et al. CoZn nanoparticles@hollow carbon tubes enabled high-performance potassium metal batteries. *ACS Appl Mater Interfaces.* **2022**;14(40):45364–72.
161. Sun L, Campbell MG, Dincă M. Electrically conductive porous metal–organic frameworks. *Angew Chem Int Ed.* **2016**;55:3566–79.
162. Xie LS, Skorupskii G, Dincă M. Electrically conductive metal–organic frameworks. *Chem Rev.* **2020**;120:8536–80.
163. He JH, Kong HY, Yang RR, Dou H, Faraz N, Wang L, et al. Review on fiber morphology obtained by bubble electrospinning and blown bubble spinning. *Therm Sci.* **2012**;16:1263–79.

164. He JH. Effect of temperature on surface tension of a bubble and hierarchical ruptured bubbles for nanofiber fabrication. *Therm Sci.* **2012**;16:327–30.
165. Yang R, He J, Xu L, Yu J. Bubble-electrospinning for fabricating nanofibers. *Polymer.* **2009**;50:5846–50.

Publisher's Note Springer Nature remains neutral with regard to jurisdictional claims in published maps and institutional affiliations

Springer Nature or its licensor (e.g. a society or other partner) holds exclusive rights to this article under a publishing agreement with the author(s) or other rightsholder(s); author self-archiving of the accepted manuscript version of this article is solely governed by the terms of such publishing agreement and applicable law.

Shunyu Yao is a Ph.D. student at the Harbin Institute of Technology in Prof. Gang Chen's group. She is also an exchange Ph.D. student at the National University of Singapore in 2021. Her research focuses on the targeted synthesis of transition metal and metal-organic framework compounds with surface interface regulation and their applications in energy conversion. Her research works have been reported in

Nano-Energy, Applied Catalysis B: Environmental, Chemical Engineering Journal, ACS Sustainable Chemistry & Engineering, and Journal of Colloid and Interface Science, respectively. Cited time of the publications is over 1300 and H-factor is 17.

Seeram Ramakrishna is a world-renowned poly-disciplinary scholar at the National University of Singapore. He is named among the World's Most Influential Minds (Thomson Reuters) and Top 1% Highly Cited Researchers in material science as well as cross-field categories (Clarivate Analytics). His publications to date have an H-index of 177 and over 151,637 citations. He is an elected Fellow of the UK Royal Academy of Engineering (FREng), AAAS, ASM International, ASME, and AIMBE, USA.

Gang Chen obtained his Ph.D. degree in Materials System from Toyohashi University of Technology in 1996. Then he was promoted to Professor in the Department of Materials Chemistry, Harbin Institute of Technology, in 1996. His main research interests are in the fields of energy conversion functional materials, including lithium-ion battery materials, nanomaterials, light-responding materials, mesoporous functional materials, and the corresponding theoretical simulations and calculations.